

Eocene to Oligocene vegetation and climate in the Tasmanian Gateway region controlled by changes in ocean currents and $p\text{CO}_2$

Michael Amoo¹, Ulrich Salzmann¹, Matthew J. Pound¹, Nick Thompson¹, and Peter K. Bijl²

¹ Department of Geography and Environmental Sciences, Northumbria University, Newcastle upon Tyne, UK

² Marine Palynology and Palaeoceanography, Utrecht University, Princetonlaan 8A, Utrecht, The Netherlands

Correspondence to: Michael Amoo (michael.amoo@northumbria.ac.uk)

Abstract. Considered as one of the most significant climate reorganisations of the Cenozoic period, the Eocene-Oligocene Transition (EOT; ca. 34.44–33.65) is characterised by global cooling and the first major glacial advance on Antarctica. While in the southern high-latitudes, the EOT cooling is primarily recorded in the marine realm, the extent and effect on terrestrial climate and vegetation is poorly documented. Here, we present a new, well-dated, continuous, high-resolution palynological (sporomorph) data and quantitative sporomorph-based climate estimates recovered from the East Tasman Plateau (ODP Site 1172) to reconstruct climate and vegetation dynamics from the late Eocene (37.97 Ma) to early Oligocene (33.06 Ma). Our results indicate three major climate transitions and four vegetation communities occupying Tasmania under different precipitation and temperature regimes: (i) a warm-temperate *Nothofagus*-Podocarpaceae dominated rainforest with paratropical elements from 37.97–37.52 Ma; (ii) cool-temperate *Nothofagus* dominated rainforest with secondary Podocarpaceae rapidly expanding and taking over regions previously occupied by the warmer taxa between 37.306–35.60 Ma; (iii) fluctuation between warm temperate - paratropical taxa and cool temperate forest from 35.50–34.49 Ma, followed by a cool phase across the EOT (34.30–33.82 Ma); (iv) post-EOT (earliest Oligocene) recovery characterised by a warm-temperate forest association from 33.55–33.06 Ma. Coincident with changes in stratification of water masses and sequestration of carbon from surface water in the Southern Ocean, our sporomorph-based temperature estimates between 37.52 Ma and 35.60 Ma (phase ii) showed 2–3 °C terrestrial cooling. The unusual fluctuation between warm and cold temperate forest between 35.50 to 34.59 Ma is suggested to be linked to the initial deepening of the Tasmanian Gateway allowing eastern Tasmania to come under the influence of warm water associated with the proto-Leeuwin Current (PLC). Further to the above, our terrestrial data show mean annual temperature declining by about 2 °C across the EOT before recovering in the earliest Oligocene. This phenomenon is synchronous with regional and global cooling during the EOT and linked to declining $p\text{CO}_2$. However, the earliest Oligocene climate rebound along eastern Tasmania is linked to transient recovery of atmospheric $p\text{CO}_2$ and sustained deepening of the Tasmanian Gateway, promoting PLC throughflow. The three main climate transitional events across the studied interval (late Eocene–earliest Oligocene) in the Tasmanian Gateway region suggest that changes in ocean circulation due to accelerated deepening of the Tasmanian Gateway may not have been solely responsible for the changes in terrestrial climate and vegetation dynamics, but a series of regional and global events, including a change in stratification of water masses, sequestration of carbon from surface waters, and changes in $p\text{CO}_2$ may have played vital roles.

35 1. Introduction

Palynological reconstruction demonstrate a high sensitivity of global vegetation to past changes in climate, leading to major shifts in biome distribution (Pound and Salzmann, 2017). The Eocene-Oligocene Transition (EOT; 34.44-33.65 Ma; Katz et al., 2008; Hutchinson et al., 2021) is one of the most important climate transitions of the Cenozoic and it is characterised by a shift from largely ice-free greenhouse conditions to an icehouse climate, involving the development of Antarctic cryosphere and global cooling (Liu et al., 2009; Pearson et al., 2009; Pagani et al., 2011; Hutchinson et al., 2021).

Tectonic opening of the southern gateways (Kennett, 1977), as well as a large and sharp drop in global atmospheric CO₂ (DeConto and Pollard, 2003; Huber et al., 2004; Zachos et al., 2008; Goldner et al., 2014; Ladant et al., 2014) have been proposed as possible drivers for this climate transition. The opening of the Australian-Antarctic Seaway (Tasmanian Gateway) and Drake Passage led to the strengthening of the Antarctic Circumpolar Current (ACC), which thermally isolated Antarctica (Kennett, 1977). However, marine geology, micropalaeontology and model simulation showed a potential time lag between the onset of the ACC and palaeogeographic changes, hence challenging a southern hemisphere tectonic driven global climate change at the EOT (Huber et al., 2004; Stickley et al., 2004; Goldner et al., 2014).

Although southern gateway opening and deepening have failed to fully explain Antarctic cooling at the EOT, the oceanographic changes following gateway opening and deepening have been reported to climatically impact Southern Ocean surface waters regionally (Stickley et al., 2004; Sijp et al., 2011; Houben et al., 2019; López-Quirós et al., 2021; Thompson et al., 2021, 2022). However, the extent and effect of the opening and deepening of the Tasmanian Gateway and its associated oceanographic changes on the coeval terrestrial climate and vegetation are not readily known. The lack of continuous and well-dated EOT terrestrial records place considerable limitations on detailed temporal and spatial reconstruction of vegetation and climate. These challenges are further compounded by the fact that the few late Eocene and early Oligocene terrestrial palynoflora records indicate a rather heterogeneous vegetation response at the EOT (Pound and Salzmann, 2017). For example, in southeastern Australia, the late Eocene to early Oligocene vegetation records indicate a shift from a warm-temperate to a cool-temperate rainforest (Korasidis et al., 2019; Lauretano et al., 2021) whereas in New Zealand, a warm humid rainforest persisted (Pocknall, 1989; Homes et al., 2015; Prebble et al., 2021). East Antarctica (Prydz Bay) saw the collapse of tall woody vegetation and their replacement by impoverished, taiga-like vegetation with dwarfed trees before the EOT during the late Eocene (Macphail and Truswell, 2004; Truswell and Macphail, 2009; Tibbett et al., 2021), whereas across the Drake Passage region major vegetation change did not take place until the early Oligocene, where there is a distinct expansion of gymnosperms and cryptogams indicating glacial expansion (Thompson et al., 2021, 2022).

To further our understanding of the timing and potential drivers of southern high-latitude terrestrial environment change at the EOT, this study presents a new sporomorph record recovered from ODP Site 1172 (Fig.1) on the East Tasman Plateau (ETP) spanning the late Eocene (37.97 Ma) to earliest Oligocene (33.06 Ma). The proximity of our study site to the Tasmanian Gateway places it in an excellent geographical position to identify potential climate or tectonic impacts on terrestrial vegetation of the Australo-Antarctica region. To further investigate potential links between the terrestrial and marine realm we also

70 compare our pollen-based quantitative climate estimates with newly published TEX₈₆-based sea-surface temperature (SST) and mean annual air temperature (MAAT_{soil}) reconstruction from the same site (Bijl et al., 2021). Our study reveals a significant terrestrial cooling ~3 Ma prior to the EOT, and a warming in the earliest Oligocene which is most likely controlled by transient rebound of atmospheric pCO₂ and sustained deepening of the Tasmanian Gateway.

2. Materials and methods

2.1. Tectonic evolution and depositional setting

75 Continental breakup and seafloor spreading between Australia and the continental blocks of Lord Howe Rise, Campbell Plateau, and New Zealand (LCNZ) started in the late Cretaceous (~75 Ma; Cande and Stock, 2004). Northward movement of Australia was propagated by rifting leading to the formation of the Tasman Sea and separation of northeastern Australia in the Paleocene (~60 Ma; Gaina et al., 1999). The series of tectonic events paved way for major ocean currents to flow along the coast of eastern Australia and Tasmania, the ETP, and South Tasman Rise (STR; Exon et al., 2004a). However, the Tasman promontory remained and separated the Australo-Antarctic gulf (AAG) from the Pacific Ocean until the late Eocene (~35.5 Ma; Stickley et al., 2004). Our study site (ODP Site 1172 on the ETP; Fig.1) is located on one of the four continental blocks sampled during ODP Leg 189 (Exon et al., 2004b). ~~Prior to the Tasman Sea break-up in the late Cretaceous (95 Ma), the ETP was part of Tasmania and STR (Royer and Rollet, 1997; Exon et al., 2004b), subsiding slowly until the late Eocene. The ETP forms an oval platform presently located~~ ~170 km southeast of Tasmania (43°57.6'S, 149° 55.7' E; Fig. 1a; Shipboard Scientific Party, 2001) at water depths of ~2620 m (Exon et al., 2004a) and enclosed by an 1800 m high seamount (Royer and Rollet, 1997). ~~Prior to the Tasman Sea break-up in the late Cretaceous (95 Ma), the ETP (which presently form an oval platform) was part of Tasmania and the STR (Royer and Rollet, 1997; Exon et al., 2004b), subsiding slowly until the late Eocene.~~ Bathymetric studies indicate that the ETP is connected to the east coast of Tasmania by the East Tasman Saddle (Royer and Rollet, 1997) which gives no indication of a deep basin in between (Hill and Exon, 2004). Dredging exercise confirms the continental origin of the of the plateau (Exon et al., 1997). However, the age of the guyot/seamount (dated as 36 Ma; Lanyon et al., 1993) disqualifies the ETP itself as the potential source of the terrestrial organic matter (Bijl et al., 2021). In addition, common Permo-Triassic reworked elements in our late Eocene–early Oligocene sporomorph assemblage likely indicate an eastern Tasmania sporomorph source, in line with the Permian–Triassic upper Parmeener Group containing terrestrial deposits and presently making up surface lithology across east Tasmania. Previous Paleocene-Eocene sporomorph assemblage presented from the ETP (ODP Site 1172) further supports an eastern Tasmania terrestrial palynomorph source (Contreras et al., 2014). 95

Lithologically, the marine sedimentary record is divided into three units: (i) shallow-marine, organic-rich middle Eocene to lower upper Eocene clay; (ii) a highly condensed middle upper Eocene to lowermost Oligocene glauconite-rich, shallow-marine silty-sandstone; (iii) lower Oligocene siliceous-rich, carbonate ooze (Stickley et al., 2004; Exon et al., 2001). Both Holes A and D of ODP Site 1172 on the East Tasman Plateau yielded EOT records and have been analysed for their pollen

100 and spore content. The age model relies on magnetostratigraphy (which has particularly clear signal in the late Eocene; Stickley et al., 2004; Fuller and Touchard, 2004) and biostratigraphy (dinoflagellate cyst, nannoplankton, and diatoms; Stickley et al., 2004; Bijl et al., 2013) as presented in Houben et al. (2019) and Bijl et al. (2021).

2.2. Study material

105 A total of 66 samples from the late Eocene to earliest Oligocene of ODP Site 1172 (37.97-33.06 Ma) were analysed for terrestrial palynomorphs to reconstruct palaeovegetation and palaeoclimate. [Raw pollen data including non-pollen palynomorphs \(NPPs\) and reworked sporomorphs are available from Zenodo data repository \(Amoo et al., 2021\).](#) These samples were prepared at the Laboratory of Palaeobotany and Palynology, Utrecht University following standard palynological processing techniques (Bijl et al., 2013). Sample processing involved treatment with 30% HCl and 38% HF and sieving residue through a 15 µm nylon mesh (Pross, 2001). The residues were mounted onto a microscope slide with glycerine gel as the mounting medium. [When analysing marine sediments such as those used in this study, sieving is a standard technique and is required to remove unwanted organic/inorganic matter, and to increase pollen concentration. To reduce the potential risk of losing small pollen grains we regularly controlled our residues sieved at 10 µm and 15 µm mesh size. We found no evidence of a selective loss of smaller pollen grains such as *Myrtaceidites* and *Sapotaceoidaepollenites cf. latizonatus*. Similar to pollen records recovered from large lakes \(diameter > 200 m\) and estuaries in Australia, our marine sporomorph record is likely to be biased towards abundant taxa in the regional vegetation, whereas sporomorphs recovered from coal, lignite, peat, and backswamp deposits are more likely to reflect local flora with higher diversity and occasional high values of underrepresented taxa \(Macphail et al., 1994\).](#)

110 The Leica DM 500 and DM 2000 LED microscopes were used to analyse two slides for each sample at x400 or x1000 magnification. Where possible, 300 fossil spores and pollen grains (excluding reworked sporomorphs) were analysed for each sample, followed by further scanning of the entire microscope slide to record rare taxa. Aside from nine samples with counts below 50 grains, overall pollen preservation and counts were generally good. Reworked sporomorphs were identified based on the thermal maturation (colour) of their outer coat (exine) and occurrence outside their known stratigraphic range. Non-pollen palynomorphs were recorded but not added to the total pollen counts. Sporomorph percentages are calculated based on the total sum of pollen and spores, excluding reworked grains, and plotted using Tilia version 2.6.1 (Fig. 2; Grimm, 1990).
120 Using Edward's and Cavalli-Sforza Chord Distance, we applied a stratigraphically constrained incremental sum-of-squares cluster analysis (CONISS, Grimm, 1987) to determine pollen assemblage zones (PZ; Fig.2). Sporomorph identification and botanical affinities (used for nearest living relative identification of fossil spores and pollen) were established using Macphail and Cantrill (2006); Macphail (2007); Truswell and Macphail (2009); Daly et al. (2011); Kumaran et al. (2011); Raine et al. (2011); Bowman et al. (2014); ~~Stevens (2017);~~ and Macphail and Hill (2018).

2.3. Bioclimatic analysis

The nearest-living relative (NLR) approach was used to estimate and reconstruct mean annual temperature (MAT), warm mean month temperature (WMMT), cold mean month temperature (CMMT) and mean annual precipitation (MAP). The bioclimatic analysis used in this study involved all pollen and spore taxa that could be related to an NLR and are listed in Table 1. The NLR is a uniformitarian approach based on the assumption that climate tolerance of extant taxa can be extended into the past. However, factors such as misidentification of fossil taxa and/or their NLRs, unresolved differences in climate tolerance between fossil taxa and their NLRs, climate tolerance of NLRs being potentially incomplete, and potential weakening in connection between fossil taxa and NLRs through deep time may pose some concerns and need to be considered prior to the application of the NLR-based climate reconstructions (Mosbrugger and Utescher, 1997; Mosbrugger, 1999; Pross, 2000; Utescher et al., 2000, 2014). Generally, these uncertainties and issues with the NLR approach increase when analysing plant remains or samples from deep-time geological records (Poole et al., 2005). To test the validity of our NLR-based climate estimates, we compare them to previous published independent botanical or geochemical proxies in the southern high-latitude spanning the late Eocene to early Oligocene (e.g., Colwyn and Hren, 2019; Houben et al., 2019; Korasidis et al., 2019; Bijl et al., 2021; Lauretano et al., 2021; Tibbett et al., 2021). Overall, these are generally in agreement and provide a certain level of confidence in the utility of the NLR-based climate estimates.

The NLR analysis in this study is combined with the probability density function (PDF). The PDF works by statistically constraining the most likely climate co-occurrence envelope for an assemblage (Harbert and Nixon, 2015; Hollis et al., 2019). Bioclimatic analysis was performed using the dismo package in R (Hijmans et al., 2017) to cross-plot the modern distribution of the NLR from the Global Biodiversity Information Facility (GBIF; GBIF, 2021) with gridding from WorldCLIM climate surface (Fick and Hijmans, 2017). The datasets are then filtered to remove multiple entries per climate grid cell, plants whose botanical affinity are vague or doubtful, redundant, and occurrences termed exotic (e.g., garden plants). Filtering was performed to avoid bias in the probability function which may likely lead to results leaning towards a particular location (Reichgelt et al., 2018). To test the robustness of the dataset, bootstrapping was applied which was followed by calculating the likelihood of a taxon that occurs at a specific climate variable using the mean and standard deviation of modern range of each taxon (Kühl et al., 2002; Willard et al., 2019). For a more detailed explanation of this method see Willard et al. (2019) and Klages et al. (2020).

2.4. Quantitative and statistical analyses

Diversity indices (rarefaction, Shannon diversity index, equitability) were generated using PAST statistical software (Hammer et al., 2001) with sample counts of ≥ 75 individuals. Rarefaction is an interpolation technique used to compare taxonomic diversity in samples of different sizes (Birks and Line, 1992; Birks et al., 2016). Rarefaction analyses using sample counts of >75 and >100 showed similar diversity trends. We however settled on counts with ≥ 75 individual grains because they offered an added advantage of filling in the gaps that would have been created if only samples with counts of ≥ 100 grains were used.

thereby increasing the resolution of the studied section. Shannon diversity index (H) is a measure of diversity which considers the number of individuals as well as number of taxa, and evenness of the species present (Shannon, 1948) H varies ranges from 0 involving vegetation communities with a single taxon to higher values where taxa are evenly distributed (Legendre and Legendre, 2012). Equitability (J) on the other hand, measures the level of abundance and how they are distributed in an assemblage. Low J values indicate the dominance of a few species in the population (Hayek and Buzas, 2010). Pollen Zones (PZ) have been defined following stratigraphically constrained analysis (CONISS; Grimm, 1987) in Tilia (Vers. 2.6.1) using total sum of squares with chord distance square root transformation (Cavalli-Sforza and Edwards, 1967). In addition, we used Detrended Correspondence Analysis (DCA; Hill and Gauch, 1980) sample scores to measure sample-to-sample variance. DCA sample scores were generated using the Vegan package (Oksanen et al., 2019) of R statistical software (R Core Team, 2019)

3. Results

3.1. Palynological results from ODP Site 1172

The late Eocene-early Oligocene samples from the East Tasman Plateau (ODP Site 1172) yielded moderate to well-preserved sporomorphs. ~~Of the 66 samples analysed, nine do not contain sufficient pollen counts and were not used in our analyses.~~ Eighty-one (81) individual sporomorph taxa were recorded from the 57 productive samples across the studied section. The sporomorph record is dominated by *Nothofagidites* spp., making between 38% to 48% of all non-reworked sporomorphs across the studied interval (Fig.2). *Podocarpidites* spp., *Myricipites harrisii*, *Cyathidites* spp., *Phyllocladidites mawsonii* and *Araucariacites australis* form significant components of the palynoflora and occur with varying frequency (Fig.2).

Based on results from rarefaction, the average diversity for the entire studied section was ~~21.0 ± 2.9~~ 20.1 ± 1.74 taxa/sample at 75 individuals. The sporomorph record, based on CONISS is grouped into four pollen zones (PZ; Fig. 2); PZ 1 (early late Eocene; 37.97-37.52 Ma), PZ 2 (late Eocene-latest Eocene; 37.30–35.60 Ma), PZ 3 (latest Eocene-earliest Oligocene 35.50–33.36 Ma), and PZ 4 (earliest Oligocene; 33.25–33.06 Ma). All the four zones consist of characteristic palynoflora assemblages that are described below. Taxa names in bracket refer to the NLR.

3.1.1. Pollen Zone 1 (37.97–37.52 Ma; 7 samples)

Pollen zone 1 is dominated by *Nothofagidites* spp. (*Nothofagus*), which accounts for ~48% of all non-reworked palynomorphs. Taxa belonging to the *Brassospora* (~28%) subgenus of *Nothofagus* make up the most abundant component, followed by *Fuscospora* (19%) and *Lophozonia* (1%), respectively. Other angiosperms (non-*Nothofagus*) on average account for 24% of all sporomorphs. These are represented, mainly in order of decreasing occurrence, by *Myricipites harrisii* (*Gymnostoma*), *Proteacidites pseudomoides* (*Carnarvonina*), *Proteacidites* spp., *Spinizonocolpites* spp. (Arecaceae), *Malvacearumpollis mannanensis* (Malvaceae), and *Malvacipollis* spp. (Euphorbiaceae). The abundance of gymnosperms is generally low

throughout PZ 1 and accounts for about 16% of all non-reworked palynomorphs. These are also represented mainly, in order of decreasing occurrence by *Podocarpidites* spp. (Podocarpaceae), *Phyllocladidites mawsonii* (*Lagarostrobos*), *Dacrydiumites praecupressinoides* (*Dacrydium*) and *Araucariacites australis* (Araucariaceae). Ferns and mosses account for about 12% of the total sporomorphs and are represented by *Cyathidites* spp. (Cyatheaceae), *Dictyophyllidites* sp. (Gleicheniaceae), *Gleicheniidites* sp. (Gleicheniaceae), *Laevigatosporites* spp. (Blechnaceae) and *Stereisporites* sp. (*Sphagnum*).

Quantitatively, sporomorph diversity for this zone based on rarefied values is 24.6 ± 1.32 species per sample at 75 individuals. With respect to the diversity indices, the yields for Shannon diversity (H) are between 2.5233 and 2.8869, averaging at 2.7557 ± 1.12 . Equitability (J) scores are set between 0.8581 and 0.9288, with an average of 0.8985 ± 0.02 (Fig. 3; Table 2).

3.1.2. Pollen Zone 2 (37.30–35.60 Ma; 27 samples)

PZ 2 sees the decline of *Nothofagidites* spp., to about 42%. The *Brassospora*-type remains the dominant *Nothofagus* subgenus, but with a substantial decline in abundance from about 28% in PZ 1 to 22% in PZ 2. The *Fuscospora* and *Lophozonia* subgenus however, accounted for 19% and 1%, respectively (Fig. 2). Other angiosperms (non-*Nothofagus*) in comparison to PZ 1 see a decline from about 24% to 17%. In order of decreasing abundance, the most significant taxa among non-*Nothofagus* angiosperms are *Myricipites harrisii* (*Gymnostoma*), *Proteacidites* spp. (Proteaceae), *Malvacearumpollis mannanensis* (Malvaceae) and *Malvacipollis* spp. (Euphorbiaceae). A sharp decline in *Proteacidites pseudomoides* (*Carnarvonia*) is coupled with the disappearance of *Spinizonocolpites* spp. (Arecaceae). Gymnosperms, on the other hand, almost doubled in relative abundance from about 16% in PZ 1 to over 29% in PZ 2. Gymnosperm taxa in order of decreasing abundance are dominated by *Podocarpus* spp. *Araucariacites australis* (Araucariaceae), *Dacrydiumites praecupressinoides* (*Dacrydium*) and *Phyllocladidites mawsonii* (*Lagarostrobos*). *Microcachrydites antarcticus* (*Microcachrys*) is a taxon which first appears in this zone and forms an important component (~11%) of the gymnospermous assemblage. In addition to the above, cryptogams decline slightly in this zone accounting for roughly 10% of the total sporomorphs. The main members of this group are *Cyathidites* spp. (Cyatheaceae), *Gleicheniidites* (Gleicheniaceae) and *Laevigatosporites* spp. (Blechnaceae).

This zone has lower diversity than PZ 1. Based on rarefied values, the average diversity for PZ 2 is 20.52 ± 2.34 species per sample at 75 individuals. The results for Shannon diversity index (H) are between 2.4015–2.9997, averaging at 2.6656 ± 0.4622 . Equitability is set between 0.8278 and 0.93, with an average of 0.8886 ± 0.0304 (Fig. 3; Table 2).

3.1.3. Pollen Zone 3 (35.50–33.36 Ma; 20 samples)

Zone 3 shows a further decline in *Nothofagidites* spp. to approximately ~38%. However, the *Brassospora*-type *Nothofagus* sees a slight increase in abundance while the *Fuscospora*-type *Nothofagus* declines sharply from the peak 19% observed in PZ 2 to 12%. The *Lophozonia*-type remains stable (~1%). Other angiosperms (non-*Nothofagus*) see a slight decline and account for ~14% of all non-reworked sporomorphs. These are represented mainly by *Myricipites harrisii* (*Gymnostoma*) and *Proteacidites* spp. (Proteaceae), while *Malvacipollis* spp. (Euphorbiaceae), and *Malvacearumpollis mannanensis* (Malvaceae).

225 Another important observation in this interval is the re-appearance of *Spinizonocolpites* spp. (Arecaceae) and *Proteacidites*
pseudomoides (*Carnarvon*). However, in contrast to PZ 1, *Spinizonocolpites* spp. are not consistently present. Gymnosperms
increase slightly in this zone, accounting for ~~about~~ ~31%. The gymnosperms remain dominant with *Podocarpidites* spp.
(Podocarpaceae). However, other important taxa such as *Araucariacites australis* (Araucariaceae), *Phyllocladidites mawsonii*
(*Lagarostrobos*) and *Microcachrydites* (*Microcachrys*), decline. *Dacrydiumites praecupressinoides* (*Dacrydium*) reaches its
230 peak abundance in this zone. Cryptogams significantly increase in abundance and in order of abundance are represented by
Cyathidites spp. (Cyatheaceae), *Laevigatosporites* spp. (Blechnaceae), *Osmundacidites* (Osmundaceae), *Polypodiisporites*
radiatus (Polypodiaceae), and *Clavifera* spp. (Gleicheniaceae).

Based on rarefied values, the average diversity for this PZ is ~~21.37~~ 20.15 ± 1.81 species per sample. The results for Shannon
diversity (H) are between ~~2.44~~ 2.86 , averaging at ~~2.66~~ 2.12 . Equitability (J) is set between ~~0.82~~ 0.91 , averaging
235 at ~~0.87~~ 0.85 ± 0.02 (Fig. 3; Table 2).

3.1.4. Pollen Zone 4 (33.25–33.06 Ma; 3 samples)

The percentage abundance of *Nothofagidites* spp. (*Nothofagus*) including *Brassospora* (~23%), *Fuscospora* (12%) and
Lophozonia-types remain unchanged, whereas other angiosperms percentages increase substantially from 14% in PZ 3 to
~20%. In order of decreasing abundance, these are represented by *Myricipites harrisii* (*Gymnostoma*) and *Proteacidites*
240 *pseudomoides* (*Carnarvon*). PZ 4 also sees the emergence of new angiosperms such as *Sapotaceoidaepollenites cf.*
latizonatus (Sapotaceae) and *Parsonsidites psilatus* (*Parsonsia*). Gymnosperms, however, see a sharp decline in this interval
accounting for about 21% of total sporomorph taxa with *Podocarpidites* spp. (Podocarpaceae) and *Dacrydium*
praecupressinoides (*Dacrydium*) being the main components. *Microcachrydites antarcticus* (*Microcachrys*), *Araucariacites*
australis (Araucariaceae), *Phyllocladidites mawsonii* (*Lagarostrobos*) showed significant decline whereas cryptogams
245 increase to ~20%. The cryptogams are represented, in order of decreasing abundances by *Cyathidites* spp. (Cyatheaceae),
Laevigatosporites spp. (Blechnaceae), *Dictyophyllidites* sp. (Gleicheniaceae) and *Cibotiidites tuberculiformis* (Schizaeaceae).

Average diversity (21.16 ± 1.37 species per sample) is slightly ~~lower~~ ~~higher~~ than in PZ 3. The results for Shannon diversity
(H) are between 2.42–2.72, averaging at 2.54 ± 0.15 . Equitability (J) is set between 0.80–0.87, averaging at 0.83 ± 0.03 (Fig.
3.; Table 2).

250 4. Discussion

4.1. Vegetation composition and altitudinal zonation

Throughout the studied section, abundant *Nothofagidites* spp. with common *Podocarpidites* spp. *Myricipites harrisii* and
Phyllocladidites mawsonii indicate the presence of *Nothofagus*-dominated temperate rainforest (Truswell and Macphail, 2009;
Bowman et al., 2014) that likely grew across lowland and mid-altitude elevations in eastern Tasmanian. The occurrence of

255 *Araucariacites australis*, *Microcachrydites antarcticus*, and *Proteacidites parvus* may also suggest a component of the
sporomorph assemblage reflect higher altitudes with more open forest conditions (Macphail, 1999; Kershaw and Wagstaff,
2001). In addition, pollen taxa belonging to *Arecaceae*, *Gymnostoma*, and *Carnarvonia*, indicate the existence of a paratropical
vegetation community that grew in sheltered lowland and coastal areas (Huurdeeman et al., 2021). The paratropical rainforest
likely occupied lowlands and coastal areas while temperate rainforest likely grew at higher elevation, similar to vegetation
260 communities that prevailed on Wilkes Land and Tasmania during the early to mid-Eocene (Pross et al., 2012; Contreras et al.,
2013, 2014). The existence of different vegetation communities, whose NLRs today grow under different temperatures and
elevations, suggest that vegetation across eastern Tasmania were subject to climatic gradients related to differences in elevation
and/or distance to the coastline. This is supported by reports of a topographic divide between sites facing the cool Tasman
current (Gippsland basin, eastern Tasmania) and the westerly located south Australian basins (Holdgate et al., 2017) that may
265 have served as the location for higher altitude temperate forest taxa. The following sub-sections further describe each of these
vegetation communities in detail.

4.1.1. Lowland to mid-altitude *Nothofagus-Podocarpus* rainforest

Abundant *Nothofagidites* spp. with common *Podocarpidites* spp., *Myricipites harrisii*, and *Phyllocladidites mawsonii* and
Cyatheaaceae give an indication of a lowland to mid-altitude *Nothofagus-Podocarpus* dominated rainforest thriving under high
270 precipitation regimes (MAP > 1300 mm/yr) in Tasmania during the late Eocene to the earliest Oligocene. The main canopy is
primarily made up *Nothofagidites* spp. (*Nothofagus*/southern beech) and Podocarps (*Dacrydiumites*, *Podocarpidites*,
Dacrycarpites) with rare Cupressaceae trees. Southern beech forests can either occur as pure stands or a mixed forest, making
the definition and recognition of regional or local forest types from fossil pollen and spore challenging. Today, pure beech
stands in New Zealand are mostly montane to subalpine, and lowland mixed beech forests are associated with diverse broadleaf
275 angiosperms and canopy-emergent gymnosperms (Ogden et al., 1996). Following Dettmann et al. (1990), we categorise
Nothofagidites pollen taxa into the *Brassospora*, *Fuscospora* and *Lophozonia* subgenera. Extant *Fuscospora* and *Lophozonia*-
types thrive in cool temperate conditions in Tasmania, southeastern Australia, New Zealand, and southern South America
(Hill, 1994, 2017; Veblen et al., 1996; Read et al., 2005) while the *Brassospora*-type are today restricted to warm temperate-
subtropical conditions in New Guinea and New Caledonia (Hill and Dettmann, 1996; Veblen et al., 1996). These *Brassospora*-
280 type *Nothofagus* grow today at lower to mid altitudes that receive high and consistent rainfall but, also in montane and
subalpine areas (typically above 500m), pointing to their wide ecological and climate tolerance (MAT: 10.6 to 23.5 °C; Read
et al., 2005).

Myricipites harrisii (Casuarinaceae) has two potential NLR, *Casuarina/Allocasuarina* and *Gymnostoma*.
Casuarina/Allocasuarina have xeromorphic features indicating adaptation to arid climate with frequent fires (Hill, 2017; Lee
285 et al., 2016; Hill et al., 2020). We selected the rainforest clade *Gymnostoma* as the most likely NLR of our fossil taxon
Myricipites harrisii based on the subtropical affinities of the associated palynoflora. This is also supported by Paleogene

vegetation reconstruction of southeastern Australia based on macrofossil remains which indicate rainforest communities (Christophel et al., 1987; Macphail et al., 1994; Hill, 2017) with *Gymnostoma* being common from the Paleocene to Oligocene and later being replaced by *Casuarina/Allocasuarina* (sclerophyll taxa) in the Miocene (Evi et al., 1995; Boland et al., 2006; Holdgate et al., 2017); [Hill et al., 2020](#)).

Dacrydium cupressinum is suggested as the most likely NLR of *Dacrydiumites praecupressinoides* (Rimu; Raine et al., 2011). Today, *Dacrydium cupressinum* occur as a minor component in the Kauri Forest of Northland, New Zealand and occur as emergent taxa commonly associated with *Agathis australis* (Araucariaceae) and *Podocarpus totara* (Farjon, 2010). The NLR of *Phyllocladites mawsonii*, *Lagarostrobos franklinii* (Tasmanian Huon Pine; Raine et al., 2011) is very abundant at Site 1172. *Lagarostrobos* are evergreen cool temperate riparian trees that grow in Tasmania close to riverbanks (Farjon, 2010; Hill, 1994, 2017). Apart from forming groves that mark stream courses in low altitudes (Hill and Macphail, 1983; Farjon, 2010), they may also be found away from water courses on wet hillsides in temperate forest (Farjon, 2010; Bowman et al., 2014).

[Lagarostrobos is one of the most common gymnosperms at ODP Site 1172, and its percentage abundance is similar to those recovered from well offshore Gippsland Basin \(Groppe-1, Mullet-1, and Bluebone-1 wells; Partridge, 2006\). Lagarostrobos occurs with even higher percentages in the Middle *Nothofagidites asperus* Zone of the terrestrial record of the Gippsland Basin where it appears to be overrepresented \(Holdgate et al., 2017\).](#)

The two possible NLR relatives for *Proteacidites pseudomoides* are *Carnarvonia* and *Lomatia*. *Carnarvonia* thrives in warm temperate to paratropical areas such as wet northeastern Australia (Mabberley, 1997; Cooper and Cooper, 2004) and grows into large trees (Hyland, 1995). *Lomatia* grows as shrubs and small trees in remnant gallery warm temperate rainforests for example, along creek lines on sandstones in Northern Sydney (Bowman et al., 2014; Myerscough et al., 2007). *Carnarvonia* is selected as the likely NLR relative because of their significant increase in intervals where warmth-loving taxa such as *Arecaceae*, *Brassospora*-type *Nothofagus*, *Gleicheniaceae*, and *Cyatheaceae* thrive.

4.1.2. High altitude temperate rainforest and shrubland

Components of the palynoflora that reflect higher altitude and more open vegetation on soils with low fertility are *Araucariacites australis*, *Proteacidites parvus*, and *Microcachrydites antarcticus* (Kershaw and Wagstaff, 2001; Macphail et al., 1999). Today, Araucariaceae trees grow in cool temperate forests in Chile and Argentina and extend to the tree line (Veblen et al., 1996; Sanguinetti and Kitzberger, 2008). In the Andes, trees belonging to Araucariaceae are found ~~in~~at altitudes of 600-800 m a.s.l and they receive high amounts of annual rainfall (2000-3000 mm/yr) as well as experiencing hot and dry spells in summer (Farjon, 2010). Araucariaceae build pure stands at higher altitude or mixed Valdivian rainforest at lower altitudes (Farjon, 2010). Increase in araucarian sporomorph taxa between 37.30–35.60 Ma in Tasmania give an indication of a dense, emergent cover of Araucariaceae thriving in relatively dry environments (Kershaw and Wagstaff, 2001). *Microcachrys* (Raine et al., 2011), the nearest living relative of *Microcachrydites antarcticus* is a creeping shrub that grows in alpine/subalpine areas and are today restricted to western Tasmania under boreal to cool temperate conditions (Truswell and Macphail, 2009;

320 Biffin et al., 2012; Carpenter et al., 2011). Therefore, increase in this Tasmanian endemic alpine shrub (*Microcachrys*) from
37.30-35.60 Ma together with *Bellendena* (low-growing protea shrub; NLR of *Proteacidites parvus*), and Araucariaceae
(emergent canopy) suggest that the vegetation thriving in the higher altitudes in Tasmania preferred cool temperate conditions.

4.2. Subtropical vegetation and early-late Eocene cooling from 37.97-35.60 Ma

325 Throughout PZ 1 (37.97–37.52 Ma), abundant *Nothofagus* (especially *N. brassii*-type) with secondary Podocarpaceae,
Gymnostoma, along with minor Arecaceae, *Carnarvon*, and cryptogams suggest the presence of a temperate *Nothofagus*-
dominated rainforest with subtropical elements. Sporomorph-based climate estimates indicate these forests grew under MAT
between 14.2–15.1 °C and a MAP of 1467–1681 mm/yr (Fig. 4). The vegetation-based summer temperature reconstructions
of ca. 18.5 °C closely corroborate the brGDGT-biomarker reconstructions from the same site (Bijl et al., 2021), supporting the
notion of a potential seasonal bias of this palaeothermometer (Contreras et al., 2014; Naafs et al., 2017). The warmth-loving
taxa formed the main lowland forest components occupying sheltered areas and lowland subtropical coastal zones (Dowe,
330 2010; Carpenter et al., 2012; Tripathi and Srivastava, 2012; Verma et al., 2020) and swamps (Kershaw, 1988). Sporomorph-
based temperature estimates yield cold month mean temperature (CMMT) well above freezing (11.2–12.5 °C; Fig. 4). The
decline and to a large extent, the absence of cool-temperate taxa coupled with persistent warm temperate (12–17 °C; Emanuel
et al., 1985) to subtropical taxa (17–24 °C; Emanuel et al., 1985) taxa, further points to the expansion of warm temperate –
paratropical rainforest up into the mid-altitudes and uplands.

335 The *Nothofagus*-dominated rainforest continued into PZ 2 (37.30-35.60 Ma). However, at ~37.30 Ma, a distinct environmental
change occurred, leading to a drop and in some instances, the demise of warm-temperate and subtropical taxa (*Nothofagus*
subgenus *Brassospora*, *Carnarvon*, Arecaceae; Fig. 2). This vegetation change continued throughout PZ 2 with a
concomitant rise in relative abundance of *Lagarostrobos*, *Microcachrys*, and decline in diversity (Table 2) ~3 Ma prior to the
EOT. The increased occurrence of microthermal taxa points to a cool-temperate (southern beech) dominated rainforest with
secondary Podocarpaceae expanding into lowland regions previously occupied by mesothermal taxa. The late Eocene cool
340 temperate *Nothofagus*–Podocarpaceae dominated rainforest have been suggested to resemble modern Valdivian rainforest of
Chile (Veblen, 1982; Cantrill and Poole, 2012; Bowman et al., 2014), cool temperate *Nothofagus* dominated rainforest with
riparian *Lagarostrobos* restricted to river gullies in Victoria, Australia (Read and Hill, 1985) or on fertile soils in lowland
Tasmania (Read and Hill, 1985; Macphail, 2007; Francis et al., 2008).

345 This interpretation is reflected in our sporomorph-based MAT estimates indicated by a 2-3 °C decline in MAT (Fig.4). Our
findings also corroborate previous late Eocene studies throughout Australia indicating an increase in *Nothofagus* subgenus
Fuscospora with substantial decline in *Brassospora*-type *Nothofagus*, demise of most Proteaceae, Arecaceae, and most
Australian [angiospermangiosperms](#) (Kemp, 1978; Kershaw, 1988; Christophel and Greenwood, 1989; Truswell, 1993; Martin,
1994, 2006; Macphail et al., 1994; Partridge and Dettmann, 2003; Korasidis et al., 2019). In line with the vegetation change,
350 biomarker-based reconstruction from Site 1172 also indicates declining SSTs by ca. 2-3 °C starting around 37.5 Ma (Fig.4).

However, the cooling indicated by both independent proxies is not reflected by the lipid biomarker-based terrestrial MAT estimates and the reason for this disparate trend remains unknown.

The transition from a warm-temperate rainforest with paratropical elements to cool temperate forests in the Tasmanian Gateway region also matches an early-late Eocene cooling (37.3 Ma) in the Southern Ocean (Kerguelen Plateau) ~3 Ma prior to the EOT (Villa et al., 2008, 2014; Scher et al., 2014). The 2–3 °C sporomorph-based MAT (100–200 kyr) cooling around 37.3 Ma coincides with a regional transient (~140 kyr) cooling event at ODP Site 738 (Kerguelen Plateau) known as the Priabonian Oxygen Maximum (PrOM; Scher et al., 2014). The PrOM event, placed within magnetochron C17n.1n of the late Eocene, points to the temporary growth of ice sheets on East Antarctica based on positive excursion in benthic $\delta^{18}\text{O}$ (Scher et al., 2014). However, on the Kerguelen Plateau, differences in neodymium isotopic composition (ϵ_{Nd}) between bottom waters and terrigenous sediments point to changes in sediment provenance as opposed to changes in reorganisation of ocean currents (Scher et al., 2014). The transient 2–3 °C sporomorph-based MAT cooling phase is followed by a period of sustained cooler climate from 37.2 Ma to 35.6 Ma (Fig.4). This sustained cooler climate may have led to the climate threshold of the frost-sensitive (subtropical) taxa being exceeded, hence their continued decline and demise. In the marine realm, endemic-Antarctic dinoflagellate cyst (e.g., *Deflandrea antarctica*, *Vozzhennikovia* spp., and *Enneadocysta dictyostila*) become dominant at Site 1172 (Fig. 3; Stickley et al., 2004; Houben et al., 2019). The dominant endemic-Antarctic dinocyst in addition to general sea surface circulation models (Huber et al., 2004) point to the East Tasman Plateau and east Tasmania being bathed by relatively cool Antarctic-derived surface waters (Houben et al., 2019) which is consistent with TEX₈₆-based sea surface temperature records (~3–4 °C cooling; Houben et al., 2019; Bijl et al., 2021). Regionally, this sustained cool-temperate terrestrial MATs matches Oligotrophic conditions associated with low nutrients, stratification of water mass, and increase in efficiency of ocean biologic pump, which favoured cooling as a result of carbon being sequestered from surface water in the Southern Ocean (Villa et al., 2008, 2014).

Close to the top of PZ 2 (35.7 Ma; Fig.4), branched GDGT-based MATs and SSTs show strong and rapid cooling, which is not mirrored by the pollen-based climate estimates. However, strong fluctuations of gymnosperms and an increase in cryptogams (Fig.2 and Fig.3) and diversity towards the top of PZ 2 indicate increasing environmental disturbance that might be linked to their recorded change in lipid biomarkers. The rapid cooling most likely created gaps within the canopy triggering an expansion of cryptogams. The divergence between the different proxy signals could be related to their different origins and transport mechanisms. Whereas the lipid biomarkers are strongly controlled by the depositional settings, including river run-off, tectonic and geographic evolution (Bijl et al., 2021), the terrestrial palynological signal mainly ~~eonsist~~consists of wind-dispersed pollen and spores. The long distance between the study site (ODP Site 1172) and mainland Tasmania (more than 100 km) in the Eocene makes a major influence of river/water transported sporomorph unlikely.

4.3. Warm and cold temperate terrestrial climate fluctuation from 35.50–34.59 Ma

PZ 3 (35.50–33.36 Ma) is characterised by a major shift in sporomorph assemblages represented by increase in *Podocarpus*, decline in *Lagarostrobos*, *Microcachrys*, Araucariaceae and *Fusca-type Nothofagus*, with the re-emergence of subtropical and

Formatted: Font: +Body (Times New Roman)

385 warm-temperate taxa. The peak in tree ferns, especially Cyatheaceae, indicate a period of disturbance (Vajda et al., 2001)
within this interval of ~~shift in vegetation-vegetation shift. However, we are not able to attribute the disturbance within this~~
~~period (35.50-34.59 Ma) to an increase in fire frequencies due to the absence of charcoal particles within our records.~~
Sporomorph-based temperature reconstructions indicate several fluctuations between warm and cool climate phase with MAT
between 10.6–15.3 °C (Fig.4). In the regional Australo-Antarctic area, a similar phase of warming and cooling is observed in
390 the late Eocene (35.8–34.7 Ma) climate records of Prydz Bay (Passchier et al., 2017; Tibbett et al., 2021) and Southern
Australia (Benbow et al., 1995). Again, pollen-based WMMTs at Site 1172 closely match lipid biomarker derived MATs
(Fig.4). Our sporomorph-based warm and cool climate fluctuation phase between 35.50 to 34.59 Ma in comparison, is recorded
as a recovery phase in lipid biomarker-based MAT reconstruction. The fluctuations of pollen-based temperature estimates may
be at least partly caused by the proxy method that relies on presence-absence data. However, a more detailed proxy comparison
is hampered by the relative low resolution of the lipid biomarker in PZ 3.

395 Expansion and restriction of cool-temperate and warm-temperate forests which indicate cooling and warming phases are
consistent with previous late Eocene geochemical, sedimentological, and palynological studies reporting an increase in sea
surface temperature (TEX₈₆-based SST; Houben et al., 2019; Bijl et al., 2021), widespread deposition of glauconite (Stickley
et al., 2004), and increase in cosmopolitan and protoperidinioid dinocyst (Fig.3; Stickley et al., 2004; Houben et al., 2019; Bijl
et al., 2021). Though the glauconitic unit is interpreted to mark deepening and current inception due to widening of the
400 Tasmanian Gateway (Stickley et al., 2004), a more recent counterargument links the deposition of the greensand to
atmospheric-forced invigorated circulation in the Southern Ocean which helped to prepare Antarctica for rapid expansion of
ice (Houben et al., 2019) and further circulation change ~2 Ma later (at the EOT). However, ocean model studies (Baatsen et
al., 2016) in addressing the deposition of greensands along the south Australian margin, point to a further expansion in the
eastward throughflow into the southwest Pacific Ocean. Our sporomorph-based MAT consequently showed an average 2 °C
405 rise in temperature between 35.50 -34.59 Ma coinciding with earlier reports of the initial deepening of the Tasmanian Gateway
(Stickley et al., 2004). This is further supported by the common appearance of low-latitude cosmopolitan dinoflagellate cyst
taxa which rather than being supplied by the East Australian Current, are reported to have been sourced from the through-flow
associated with the eastward proto-Leeuwin Current (Huber et al., 2004; Stickley et al., 2004; Houben et al., 2019). These
events, coupled with ~2 °C recovery in SSTs (TEX₈₆-based; Houben et al., 2019; Bijl et al., 2021) between 35.7–34.59 Ma
410 most likely point to warm surface waters associated with the Australo-Antarctic Gulf (AAG) influencing ODP Site 1172
(Houben et al., 2019), which at this time is reported to have been close to land (eastern Tasmania; Stickley et al., 2004), thereby
affecting terrestrial climate and vegetation.

4.4. EOT cooling and climate rebound in earliest Oligocene from 34.30-33.06 Ma

415 At the onset of the EOT, our sporomorph record provides evidence for a return to a sustained cooler period on Tasmania
spanning 34.30 to 33.82 Ma. This EOT cool phase coincides with the demise of *Spinizonocolpites* sp. (Arecaceae), a drop in
Cyatheaceae and Gleicheniaceae, slight increase in *Microcachrys* and *Lagarostrobos*. The palynoflora assemblage during the

EOT is further characterized by a drop in overall angiosperm (non-*Nothofagus*) diversity with gymnosperms and *Nothofagus* (*Brassospora*-type) being common and co-dominating. Previous studies in southeast Australia (e.g., Macphail et al., 1994; Benbow et al., 1995; Holdgate et al., 2017; Lauretano et al., 2021) record a contemporaneous drop in angiosperm diversity and the final demise in Arecaceae (thermophilous elements) at the end of the Eocene (Pole and Macphail, 1996; Martin, 2006). Quantitatively, our sporomorph-based MAT reconstruction records a ~2 °C decline across the EOT (Fig.4) which coincides with ~2.4 °C and 5 °C cooling step in southeastern Australia (MBT⁵me-based MAATsoil; Lauretano et al., 2021) and East Antarctica (Prydz Bay; MBT⁵me-based MAATsoil; Tibbett et al., 2021) respectively. This cooling in our terrestrial record further matches the principal geochemical signature of EOT in the marine realm, which is ~ +1.5‰ excursion of oxygen isotope ratio of deep-sea benthic foraminifera (Zachos et al., 1996; Coxall et al., 2005; Pälike et al., 2006; De Vleeschouwer et al., 2017; Fig.5) associated with global cooling (Zanazzi et al., 2007; Pearson et al., 2009; Pagani et al., 2011; Hutchinson et al., 2021; Tibbett et al., 2021). This cooling at the EOT have been linked to global decline in atmospheric *p*CO₂ (Pearson et al., 2009; Lauretano et al., 2021)

Between ~33.25 – 33.06 Ma (PZ 4), the sporomorph-based climate estimates indicate a warming with MATs between 12.7-15.3 °C (Fig.4). In addition, the presence of warmth-loving taxa notably Sapotaceae, *Parsonsia* (Silkpod), and Polypodiaceae (subtropical epiphytes) further indicate a warming phase. The pollen flora resembles Oligocene warm-temperate *brassii* southern beech dominated forests of Karamu in the Waikato coal measures of New Zealand (Pocknall, 1985). The increase of *brassii*-type *Nothofagus* coupled with the appearance of Sapotaceae, and subtropical epiphytes suggests that, at least locally on lowlands, eastern Tasmania was warm enough to accommodate warm-temperate vegetation in the earliest Oligocene. Previous earliest Oligocene studies in Southeast Australia (Korasidis et al., 2019) show the presence of a cool temperate rainforest community. The palynoflora on east Antarctica (Askin, 2000; Askin and Raine, 2000; Prebble et al., 2006; Tibbett et al., 2021) and northeast Tasmania (Hill and Macphail, 1983) suggest an early Oligocene cold-temperate *Nothofagus* (subgenus *Lophozonia* or *Fuscospora*)-Podocarpaceae vegetation. These northern Tasmania and east Antarctica palynoflora are however reported to have most likely been made up of prostrate deciduous dwarf trees (Francis and Hill, 1996) or small stature closed southern beech/podocarp refugia with a vegetation community that likely struggled to survive (Askin, 2000; Askin and Raine, 2000; Prebble et al., 2006; Francis et al., 2008; Tibbett et al., 2021). However, rather than a regional scrub (e.g., in Antarctica), the slight increase in angiosperms (other than *Nothofagus*) and cryptogams point to a local warm temperate forest growing along eastern Tasmania in the earliest Oligocene. Today, temperate forests in New Zealand and Tasmania host a diverse range of cryptogams as compared to scrub communities that do not offer other taxa to thrive under the low, closed canopies (Prebble et al., 2006).

Terrestrial cooling observed across the EOT followed by rapid recovery in the earliest Oligocene matches a partial return to warmer temperatures in previously reported terrestrial (Colwyn and Hren, 2019; Lauretano et al., 2021) and marine studies (Katz et al., 2008; Lear et al., 2008; Liu et al., 2009; Houben et al., 2012). The synchronicity between terrestrial and marine records suggest that, in addition to localised events (sustained Tasmanian Gateway deepening and widening; Stickley et al., 2004), the EOT and earliest Oligocene ETP record may also be responding to a much wider regional or global event. The most

common explanation for global cooling (Zanazzi et al., 2007; Pagani et al., 2011; Hutchinson et al., 2021; Tibbett et al., 2021) across the EOT and transient warming in the earliest Oligocene have been ascribed to the decline in concentration of atmospheric carbon dioxide ($p\text{CO}_2$) and its recovery or rebound in the earliest Oligocene respectively (Pearson et al., 2009; Heureux and Rickaby, 2015; Anagnostou et al., 2016; Fig. 5). Our results suggest that the warming, or at least the lack of sustained cooling following the EOT in eastern Tasmania, may be related to a combination of $p\text{CO}_2$ recovery (Pearson et al., 2009) coupled with sustained Tasmanian gateway deepening and widening (Stickley et al., 2004; Houben et al., 2019) allowing the influx of more warm surface waters from AAG into the southwest Pacific thereby affecting terrestrial climate and vegetation along eastern Tasmania.

5. Conclusions

The late Eocene–early Oligocene vegetation reconstructed from terrestrial palynomorphs recovered from ODP Site 1172 (East Tasman Plateau) is characterised by three major climate transitions.

- 1) The early-late Eocene sporomorph record suggests a distinct 2–3 °C terrestrial cooling at 37.30 Ma coupled with a transition from a warm-temperate *Nothofagus*-Podocarpaceae dominated rainforest with paratropical elements to a cool-temperate *Nothofagus* dominated rainforest with secondary Podocarpaceae. This terrestrial cooling at 37.30 Ma and sustained cool climate from 37.2–35.60 Ma coincides with long term SST decline from ~23 to 19 °C at ODP Site 1172, regional transient cooling event (PrOM) at ODP Site 738 (Kerguelen Plateau; Scher et al., 2014), and a relatively long-term regional Southern Ocean cooling due to carbon being sequestered from surface water (Villa et al., 2008, 2014).
- 2) Expansion and restriction of cool and warm temperate forests from 35.5–34.49 Ma, followed by a period of cooling across the EOT (34.30–33.82 Ma). This terrestrial climate fluctuation in this zone is consistent with latest Eocene geochemical, sedimentological and palynological studies reporting an increase in SST, recovery in MBT^{5me}-based MAATsoil (biomarker thermometry), widespread deposition of glauconite and common occurrence of low-latitude cosmopolitan and protoperidinioid dinocyst. These are interpreted to be linked to the initial deepening of the Tasmanian Gateway paving way for the warm water associated with the PLC to affect both terrestrial and marine climate in this region.
- 3) Post-EOT (earliest Oligocene) recovery characterised by a warm-temperate forest association from 33.55–33.06 Ma. This earliest Oligocene recovery in Tasmanian terrestrial temperatures following prior cooling across the EOT coincides with rebound of atmospheric $p\text{CO}_2$ at the earliest Oligocene glacial maximum (EOGM; Pearson et al., 2009) coupled with icesheet expansion in Antarctica (Galeotti et al., 2016), and sustained deepening of the Tasmanian Gateway (Stickley et al., 2004).

Our study shows that, against backdrop of global cooling in the late Eocene (sustained decline in $p\text{CO}_2$), a series of regional events in the marine realm, including a change in stratification of water masses, sequestration of carbon from surface water

and, changes in ocean circulation due to Tasmanian Gateway accelerated deepening may have had a knock-on effect in driving terrestrial climate and vegetation change in the Tasmanian Gateway region.

485 **6. Data availability**~~Author contributions~~

All data are available for download from the Zenodo data repository at <https://doi.org/10.5281/zenodo.5924930> (Amoo et al., 2021).

7. Author contributions

490 MA and US conceived, designed and led this study. PKB supplied the palynological samples for this study and provided the biomarker thermometry data. MA and US undertook palynological analyses. MA interpreted palynological data and performed sporomorph-based bioclimatic analyses. MJP and NT provided guidance and expertise with pollen-based palaeoenvironmental reconstruction. MA prepared the manuscript with contributions from ~~all co-authors~~ US, PKB, MJP, and NT.

7.8. Competing interests

The authors declare that they have no conflict of interest.

495 **7.9. Acknowledgements**

Samples for this study were supplied by the Ocean Drilling Program (ODP) sponsored by the US National Science Foundation under the management of the Joint Oceanographic Institutions (JOI). ~~MA acknowledges~~ Dr. Florian Schwarz is thanked for providing technical support regarding sporomorph-based climate estimate calculations. The authors thank Dr Ian Sluiter and an anonymous reviewer for their helpful comments that have greatly improved our manuscript.

500 **10. Financial support**

Michael Amoo received funding from Northumbria University Research Development Fund (RDF). ~~NT~~ Nick Thompson received funding from the Natural Environment Research Council (NERC)-funded Doctoral Training Partnership ONE Planet [NE/S007512/1]. ~~PKB~~ Peter K. Bijl acknowledges funding from the European Research Council for starting grant ~~#number~~ 802835, OceaNice.

505 **911. References**

[Amoo, M., Salzmann, U., Pound, J. M., Thompson, N. and Bijl, K. P.: Eocene to Oligocene vegetation and climate in the Tasmanian Gateway region controlled by changes in ocean currents and pCO₂ \[data set\]. *Climate of the Past*, Zenodo, <https://doi.org/10.5281/zenodo.5924930>, 2021.](https://doi.org/10.5281/zenodo.5924930)

510 Anagnostou, E., John, E. H., Edgar, K. M., Foster, G. L., Ridgwell, A., Inglis, G. N., Pancost, R. D., Lunt, D. J. and Pearson, P. N.: Changing atmospheric CO₂ concentration was the primary driver of early Cenozoic climate, *Nature*, 533(7603), 380–384, doi:10.1038/nature17423, 2016.

Askin, R. A.: Spores and pollen from the McMurdo Sound Erratics, Antarctica, in *Paleobiology and Paleoenvironments of Eocene Rocks, McMurdo Sound, East Antarctica*, vol. 76, edited by J. D. Stillwell and R. M. Feldmann, pp. 161–181, American Geophysical Union Antarctic Research Series., 2000.

515 Askin, R. A. and Raine, J. I.: Oligocene and Early Miocene Terrestrial Palynology of the Cape Roberts Drillhole CRP-2/2A, Victoria Land Basin, Antarctica, *Terra Antarct.*, 7(4), 493–501, 2000.

Baatsen, M., Van Hinsbergen, D. J. J., Von Der Heydt, A. S., Dijkstra, H. A., Sluijs, A., Abels, H. A. and Bijl, P. K.: Reconstructing geographical boundary conditions for palaeoclimate modelling during the Cenozoic, *Clim. Past*, 12(8), 1635–1644, doi:10.5194/cp-12-1635-2016, 2016.

520 Benbow, M. C., Alley, N. F., Callan, R. A. and Greenwood, D. R.: *Geological history and palaeoclimate*, edited by J. F. Dixel and W. V. Preiss, pp. 208–217, Adelaide., 1995.

Biffin, E., Brodribb, T. J., Hill, R. S., Thomas, P. and Lowe, A. J.: Leaf evolution in Southern Hemisphere conifers tracks the angiosperm ecological radiation, *Proc. R. Soc. B Biol. Sci.*, 279(1727), doi:10.1098/rspb.2011.0559, 2012.

525 Bijl, P. K., Bendle, J. A. P., Bohaty, S. M., Pross, J., Schouten, S., Tauxe, L., Stickley, C. E., McKay, R. M., Rohlf, U., Olney, M., Sluijs, A., Escutia, C. and Brinkhuis, H.: Eocene cooling linked to early flow across the Tasmanian Gateway, *Proc. Natl. Acad. Sci. U. S. A.*, 110(24), 9645–9650, doi:10.1073/pnas.1220872110, 2013.

Bijl, P. K., Frieling, J., Cramwinckel, M. J., Boschman, C., Sluijs, A. and Peterse, F.: Maastrichtian–Rupelian paleoclimates in the southwest Pacific – a critical re-evaluation of biomarker paleothermometry and dinoflagellate cyst paleoecology at Ocean Drilling Program Site 1172, *Clim. Past* ~~*Discuss.*~~, 2021, ~~1–82~~, [17\(6\), 2393–2425](https://doi.org/10.5194/cp-17-2393-2021), doi:10.5194/cp-17-2393-2021 ~~18~~, 2021.

530 Birks, H. J. B. and Line, J. M.: The use of rarefaction analysis for estimating palynological richness from Quaternary pollen-analytical data, *The Holocene*, 2(1), 1–10, doi:10.1177/095968369200200101, 1992.

Birks, H. J. B., Felde, V. A., Bjune, A. E., Grytnes, J. A., Seppä, H. and Giesecke, T.: Does pollen-assemblage richness reflect floristic richness? A review of recent developments and future challenges, *Rev. Palaeobot. Palynol.*, 228, 1–25, doi:10.1016/j.revpalbo.2015.12.011, 2016.

Boland, D., Brooker, M., Chippendale, G., Hall, N., Hyland, B., Johnston, R., Kleinig, D., McDonald, M. and Turner, J.: *Forest trees of Australia*, 5th ed., CSIRO, Melbourne., 2006.

535 Bowman, V. C., Francis, J. E., Askin, R. A., Riding, J. B. and Swindles, G. T.: Latest Cretaceous-earliest Paleogene vegetation and climate change at the high southern latitudes: Palynological evidence from Seymour Island, Antarctic Peninsula,

- 540 Palaeogeogr. Palaeoclimatol. Palaeoecol., 408, 26–47, doi:10.1016/j.palaeo.2014.04.018, 2014.
- Cande, S. C. and Stock, J. M.: Cenozoic reconstruction of the Australia-New Zealand-south Pacific sector of Antarctica, in *The Cenozoic Southern Ocean: Tectonics, sedimentation and climate change between Australia and Antarctica*, edited by N. F. Exon, J. P. Kennett, and M. J. Malone, pp. 5–18, Geophysical Monograph Series, American Geophysical Union., 2004.
- 545 Cantrill, D. J. and Poole, I.: After the heat: late Eocene to Pliocene climatic cooling and modification of the Antarctic vegetation, in *The Vegetation of Antarctica through Geological Time*, edited by D. J. Cantrill and I. Poole, Cambridge University Press, Cambridge., 2012.
- Carpenter, R. J., Jordan, G. J., Mildenhall, D. C. and Lee, D. E.: Leaf fossils of the ancient Tasmanian relict *Microcachrys* (Podocarpaceae) from New Zealand, *Am. J. Bot.*, 98(7), doi:10.3732/ajb.1000506, 2011.
- 550 Carpenter, R. J., Jordan, G. J., Macphail, M. K. and Hill, R. S.: Near-tropical Early Eocene terrestrial temperatures at the Australo-Antarctic margin, western Tasmania, *Geology*, 40(3), doi:10.1130/G32584.1, 2012.
- Cavalli-Sforza, L. L. and Edwards, A. W.: Phylogenetic analysis, *Am. J. Hum. Genet.*, 19, 233–257, 1967.
- Christophel, D. C. and Greenwood, D. R.: Changes in climate and vegetation in Australia during the tertiary, *Rev. Palaeobot. Palynol.*, 58(2–4), doi:10.1016/0034-6667(89)90079-1, 1989.
- 555 Christophel, D. C., Harris, W. K. and Syber, A. K.: The Eocene flora of the Anglesea Locality, Victoria, *Alcheringa An Australas. J. Palaeontol.*, 11(4), doi:10.1080/03115518708619139, 1987.
- Colwyn, D. A. and Hren, M. T.: An abrupt decrease in Southern Hemisphere terrestrial temperature during the Eocene–Oligocene transition, *Earth Planet. Sci. Lett.*, 512, 227–235, doi:10.1016/j.epsl.2019.01.052, 2019.
- Contreras, L., Pross, J., Bijl, P. K., Koutsodendrīs, A., Raine, J. I., van de Schootbrugge, B. and Brinkhuis, H.: Early to Middle Eocene vegetation dynamics at the Wilkes Land Margin (Antarctica), *Rev. Palaeobot. Palynol.*, 197, 119–142, doi:10.1016/j.revpalbo.2013.05.009, 2013.
- 560 Contreras, L., Pross, J., Bijl, P. K., O’Hara, R. B., Raine, J. I., Sluijs, A. and Brinkhuis, H.: Southern high-latitude terrestrial climate change during the Palaeocene-Eocene derived from a marine pollen record (ODP Site 1172, East Tasman Plateau), *Clim. Past*, 10(4), 1401–1420, doi:10.5194/cp-10-1401-2014, 2014.
- Cooper, W. and Cooper, W.: *Fruits of the Australian tropical rainforest*, Nokomis Publications, [Clifton Hill], Victoria., 2004.
- 565 Coxall K., H., Wilson A., P., Palike, H., Lear H., C. and Backman, J.: Rapid stepwise onset of Antarctic glaciation and deeper calcite compensation in the Pacific Ocean, *Nature*, 433(7021), 53–57, doi:10.1038/nature03135, 2005.
- Daly, R. J., Jolley, D. W., Spicer, R. A. and Ahlberg, A.: A palynological study of an extinct arctic ecosystem from the Palaeocene of Northern Alaska, *Rev. Palaeobot. Palynol.*, 166(1–2), 107–116, doi:10.1016/j.revpalbo.2011.05.008, 2011.
- 570 De Vleeschouwer, D., Vahlenkamp, M., Crucifix, M. and Pälike, H.: Alternating Southern and Northern Hemisphere climate response to astronomical forcing during the past 35 m.y., *Geology*, 45(4), 375–378, doi:10.1130/G38663.1, 2017.
- DeConto, R. M. and Pollard, D.: Rapid Cenozoic glaciation of Antarctica induced by declining atmospheric CO₂, *Nature*, 1317(2001), 245–249, doi:https://doi.org/10.1038/nature01290, 2003.
- Dettmann, M. E., Pocknall, D. T., Romero, E. J. and Zamalao, M. del C.: *Nothofagidites Erdtman ex Potonie*, 1960; a catalogue

- of species with notes on the paleogeographic distribution of *Nothofagus* Bl. (southern beech), *New Zeal. Geol. Surv. Paleontol. Bull.*, 60, 1–77, 1990.
- 575 Dowe, J. L.: *Australian Palms*, CSIRO Publishing, Victoria., 2010.
- Emanuel, W. R., Shugart, H. H. and Stevenson, M. P.: Climatic change and the broad-scale distribution of terrestrial ecosystem complexes, *Clim. Change*, 7(1), 29–43, doi:10.1007/BF00139439, 1985.
- Evi, E., Hill, R. S. and Scriven, L. J.: The angiosperm-dominated woody vegetation of Antarctica: a review, *Rev. Palaeobot. Palynol.*, 86, 175–198, 1995.
- 580 Exon, N. F., Berry, R. F., Crawford, A. J. and Hill, P. J.: Geological evolution of the East Tasman Plateau, a continental fragment southeast of Tasmania, *Aust. J. Earth Sci.*, 44(5), 597–608, doi:10.1080/08120099708728339, 1997.
- Exon, N. F., Kennett, J. P. and Malone, M. J.: *Proceedings of the Ocean Drilling Program, 189 Initial Reports, Ocean Drilling Program.*, 2001.
- 585 Exon, N. F., Kennett, J. P. and Malone, M. J.: Leg 189 synthesis: Cretaceous-Holocene history of the Tasmanian gateway, *Proc. Ocean Drill. Progr. Sci. Results*, doi:10.2973/odp.proc.sr.189.101.2004, 2004a.
- Exon, N. F., Kennett, J. P. and Malone, M. J.: *The Cenozoic Southern Ocean: Tectonics, sedimentation and climate change between Australia and Antarctica*, Geophysical Monograph Series, 151, American Geophysical Union, Washington., 2004b.
- Farjon, A.: *A handbook of the World's Conifers*, Koninklijke Brill, Leiden, The Netherlands., 2010.
- 590 Fick, S. E. and Hijmans, R. J.: WorldClim 2: new 1-km spatial resolution climate surfaces for global land areas, *Int. J. Climatol.*, 37(12), 4302–4315, doi:10.1002/joc.5086, 2017.
- Francis, J. E., Marensi, S., Levy, R., Hambrey, M., Thorn, V. C., Mohr, B., Brinkhuis, H., Warnaar, J., Zachos, J., Bohaty, S. and DeConto, R.: From Greenhouse to Icehouse - The Eocene/Oligocene in Antarctica, *Dev. Earth Environ. Sci.*, 8, 309–368, doi:10.1016/S1571-9197(08)00008-6, 2008.
- 595 Fuller, M. and Touchard, Y.: On the magnetostratigraphy of the East Tasman Plateau, timing of the opening of the Tasmanian Gateway and paleoenvironmental changes, in *The Cenozoic Southern Ocean: tectonics, sedimentation and climate change between Australia and Antarctica*, edited by N. Exon, J. P. Kennett, and M. Malone, pp. 127–151, American Geophysical Union, Geophysical Monograph series, Washington., 2004.
- Gaina, C., Müller, R. D., Royer, J.-Y. and Symonds, P.: Evolution of the Louisiade triple junction, *J. Geophys. Res. Solid Earth*, 104(B6), 12927–12939, doi:10.1029/1999JB900038, 1999.
- 600 Galeotti, S., DeConto, R., Naish, T., Stocchi, P., Florindo, F., Pagani, M., Barrett, P., Bohaty, S. M., Lanci, L., Pollard, D., Sandroni, S., Talarico, F. M. and Zachos, J. C.: Antarctic Ice Sheet variability across the Eocene-Oligocene boundary climate transition, *Science* (80-), 352(6281), 76–80, doi:10.1126/science.aab0669, 2016.
- GBIF: GBIF Occurrence Download [data set], <https://doi.org/10.15468/dl.nckq6t>, Available from: <https://www.gbif.org/occurrence/download/0009228-210914110416597> (Accessed 27 September 2021), 2021.
- 605 Goldner, A., Herold, N. and Huber, M.: Antarctic glaciation caused ocean circulation changes at the Eocene-Oligocene transition, *Nature*, 511(7511), 574–577, doi:10.1038/nature13597, 2014.

- Grimm, E. C.: CONISS: a FORTRAN 77 program for stratigraphically constrained cluster analysis by the method of incremental sum of squares, *Comput. Geosci.*, 13(1), 13–35, doi:10.1016/0098-3004(87)90022-7, 1987.
- 610 Grimm, E. C.: Tilia and Tiliagraph. PC spreadsheet and graphics software for pollen data, *INQUA Work. Gr. Data Handl. Methods, Newsl.*, 4, 5–7, 1990.
- Hammer, Ø., Harper, D. A. T. and Ryan, P. D.: Past: Paleontological statistics software package for education and data analysis, *Palaeontol. Electron.*, 4(1), 178, 2001.
- Harbert, R. S. and Nixon, K. C.: Climate reconstruction analysis using coexistence likelihood estimation (CRACLE): A method for the estimation of climate using vegetation, *Am. J. Bot.*, 102(8), 1277–1289, doi:10.3732/ajb.1400500, 2015.
- 615 Harbert, R. S. and Nixon, K. C.: Climate reconstruction analysis using coexistence likelihood estimation (CRACLE): A method for the estimation of climate using vegetation, *Am. J. Bot.*, 102(8), 1277–1289, doi:10.3732/ajb.1400500, 2015.
- Hayek, L. C. and Buzas, M. A.: *Surveying Natural Populations*, Columbia University Press, New York., 2010.
- Heureux, A. M. C. and Rickaby, R. E. M.: Refining our estimate of atmospheric CO₂ across the Eocene-Oligocene climatic transition, *Earth Planet. Sci. Lett.*, 409, 329–338, doi:10.1016/j.epsl.2014.10.036, 2015.
- Hijmans, R. J., Phillips, S., Leathwick, J. and Elith, J.: *dismo: Species distribution modelling*, R Packag. version, 1(4), 1, 2017.
- 620 Hill, M. O. and Gauch, H. G.: Detrended correspondence analysis: An improved ordination technique, *Vegetatio*, 43, 47–58, 1980.
- Hill, P. J. and Exon, N. F.: Tectonics and basin development of the offshore Tasmanian area; incorporating results from deep ocean drilling, in *The Cenozoic Southern Ocean; tectonics, sedimentation and climate between Australia and Antarctica*, edited by N. F. Exon, J. P. Kennett, and M. Malone, pp. 19–19, *Geophysical Monograph Series*, 151, American Geophysical Union, Washington., 2004.
- 625 Hill, P. J. and Exon, N. F.: Tectonics and basin development of the offshore Tasmanian area; incorporating results from deep ocean drilling, in *The Cenozoic Southern Ocean; tectonics, sedimentation and climate between Australia and Antarctica*, edited by N. F. Exon, J. P. Kennett, and M. Malone, pp. 19–19, *Geophysical Monograph Series*, 151, American Geophysical Union, Washington., 2004.
- Hill, R. S.: *History of the Australian Vegetation: Cretaceous to Recent*, edited by R. S. Hill, University of Adelaide Press., 1994.
- Hill, R. S.: *History of the Australian Vegetation: Cretaceous to Recent*, edited by R. S. Hill, University of Adelaide Press., 2017.
- 630 Hill, R. S. and Macphail, M. K.: Reconstruction of the Oligocene vegetation at Pioneer, northeast Tasmania, Alcheringa An Australas. *J. Palaeontol.*, 7(4), doi:10.1080/03115518308619613, 1983.
- Hill, S. R. and Dettmann, E. M.: Origin and diversification of the Genus *Nothofagus*, in *The Ecology and Biogeography of Nothofagus forests*, edited by T. T. Veblen, S. R. Hill, and J. Read, pp. 11–24, Yale University Press, New Haven., 1996.
- 635 [Hill, R. S., Whang, S. S., Korasidis, V., Bianco, B., Hill, K. E., Paull, R. and Guerin, G. R.: Fossil evidence for the evolution of the Casuarinaceae in response to low soil nutrients and a drying climate in Cenozoic Australia. *Aust. J. Bot.*, 68\(3\), 179–194, doi:10.1071/BT19126, 2020.](#)
- Hoem, F. S., Valero, L., Evangelinos, D., Escutia, C., Duncan, B., McKay, R. M., Brinkhuis, H., Sangiorgi, F. and Bijl, P. K.: Temperate Oligocene surface ocean conditions offshore of Cape Adare, Ross Sea, Antarctica, *Clim. Past*, 17(4), 1423–1442, doi:10.5194/cp-17-1423-2021, 2021.
- 640 Holdgate, G. R., Sluiter, I. R. K. and Taglieri, J.: Eocene-Oligocene coals of the Gippsland and Australo-Antarctic basins – Paleoclimatic and paleogeographic context and implications for the earliest Cenozoic glaciations, *Palaeogeogr. Palaeoclimatol.*

- Palaeoecol., 472, 236–255, doi:10.1016/j.palaeo.2017.01.035, 2017.
- Hollis, C. J., Dunkley Jones, T., Anagnostou, E., Bijl, P. K., Cramwinckel, M. J., Cui, Y., Dickens, G. R., Edgar, K. M., Eley, Y., Evans, D., Foster, G. L., Frieling, J., Inglis, G. N., Kennedy, E. M., Kozdon, R., Lauretano, V., Lear, C. H., Littler, K., Lourens, L., Nele Meckler, A., Naafs, B. D. A., Pälike, H., Pancost, R. D., Pearson, P. N., Röhl, U., Royer, D. L., Salzmann, U., Schubert, B. A., Seebeck, H., Sluijs, A., Speijer, R. P., Stassen, P., Tierney, J., Tripathi, A., Wade, B., Westerhold, T., Witkowski, C., Zachos, J. C., Ge Zhang, Y., Huber, M. and Lunt, D. J.: The DeepMIP contribution to PMIP4: Methodologies for selection, compilation and analysis of latest Paleocene and early Eocene climate proxy data, incorporating version 0.1 of the DeepMIP database, *Geosci. Model Dev.*, 12(7), 3149–3206, doi:10.5194/gmd-12-3149-2019, 2019.
- Homes, A. M., Cieraad, E., Lee, D. E., Lindqvist, J. K., Raine, J. I., Kennedy, E. M. and Conran, J. G.: A diverse fern flora including macrofossils with in situ spores from the late Eocene of southern New Zealand, *Rev. Palaeobot. Palynol.*, 220, 16–28, doi:10.1016/j.revpalbo.2015.04.007, 2015.
- Houben, A. J. P., van Mourik, C. A., Montanari, A., Coccioni, R. and Brinkhuis, H.: The Eocene–Oligocene transition: Changes in sea level, temperature or both?, *Palaeogeogr. Palaeoclimatol. Palaeoecol.*, 335–336, doi:10.1016/j.palaeo.2011.04.008, 2012.
- Houben, A. J. P., Bijl, P. K., Sluijs, A., Schouten, S. and Brinkhuis, H.: Late Eocene Southern Ocean cooling and invigoration of circulation preconditioned Antarctica for full-scale glaciation, *Geochemistry, Geophys. Geosystems*, 20(5), 2214–2234, doi:10.1029/2019GC008182, 2019.
- Huber, M., Brinkhuis, H., Stickley, C. E., Döös, K., Sluijs, A., Warnaar, J., Schellenberg, S. A. and Williams, G. L.: Eocene circulation of the Southern Ocean: Was Antarctica kept warm by subtropical waters?, *Paleoceanography*, 19(4), 1–12, doi:10.1029/2004PA001014, 2004.
- Hutchinson, D. K., Coxall, H. K., Lunt, D. J., Steinthorsdottir, M., De Boer, A. M., Baatsen, M., Von Der Heydt, A., Huber, M., Kennedy-Asser, A. T., Kunzmann, L., Ladant, J. B., Lear, C. H., Moraweck, K., Pearson, P. N., Piga, E., Pound, M. J., Salzmann, U., Scher, H. D., Sijp, W. P., Á liwińska, K. K., Wilson, P. A. and Zhang, Z.: The Eocene–Oligocene transition: A review of marine and terrestrial proxy data, models and model–data comparisons, *Clim. Past*, 17(1), 269–315, doi:10.5194/cp-17-269-2021, 2021.
- Hyland, B. P. M.: Carnarvonina, in *Flora of Australia*, Volume 16, Elaeagnaceae, Proteaceae 1, vol. 16, edited by P. McCarthy, pp. 343–345, CSIRO Publishing/Australian Biological Resources Study, CANBERRA., 1995.
- Katz, M. E., Miller, K. G., Wright, J. D., Wade, B. S., Browning, J. V., Cramer, B. S. and Rosenthal, Y.: Stepwise transition from the Eocene greenhouse to the Oligocene icehouse, *Nat. Geosci.*, 1(5), 329–334, doi:10.1038/ngeo179, 2008.
- Kemp, E. M.: Tertiary climatic evolution and vegetation history in the Southeast Indian Ocean region, *Palaeogeogr. Palaeoclimatol. Palaeoecol.*, 24(3), 169–208, doi:10.1016/0031-0182(78)90042-1, 1978.
- Kennett, J. P.: Cenozoic evolution of Antarctic glaciation, the circum-Antarctic Ocean, and their impact on global paleoceanography, *J. Geophys. Res.*, 82(27), 3843–3860, doi:10.1029/jc082i027p03843, 1977.
- Kershaw, A. P.: Australasia, in *Vegetation History*, edited by B. Huntley and T. Webb 111, pp. 237–306, Kluwer Academic Publishers, Dordrecht., 1988.
- Kershaw, P. and Wagstaff, B.: The southern conifer family Araucariaceae: History, status, and value for paleoenvironmental

- reconstruction, *Annu. Rev. Ecol. Syst.*, 32(1), 397–414, doi:10.1146/annurev.ecolsys.32.081501.114059, 2001.
- 680 Korasidis, V. A., Wallace, M. W., Wagstaff, B. E. and Hill, R. S.: Terrestrial cooling record through the Eocene-Oligocene transition of Australia, *Glob. Planet. Change*, 173, 61–72, doi:10.1016/j.gloplacha.2018.12.007, 2019.
- Kühl, N., Gebhardt, C., Litt, T. and Hense, A.: Probability density functions as botanical-climatological transfer functions for climate reconstruction, *Quat. Res.*, 58(3), 381–392, doi:10.1006/qres.2002.2380, 2002.
- Kumaran, N., Punekar, S. and Limaye, R.: Palaeoclimate and phytogeographical appraisal of Neogene pollen record from India, *J. Palynol.*, 46, 315–330, 2011.
- 685 Ladant, J. B., Donnadieu, Y. and Dumas, C.: Links between CO₂, glaciation and water flow: Reconciling the cenozoic history of the antarctic circumpolar current, *Clim. Past*, 10(6), 1957–1966, doi:10.5194/cp-10-1957-2014, 2014.
- Lanyon, R., Varne, R. and Crawford, A. J.: Tasmanian Tertiary basalts, the Balleny plume, and opening of the Tasman Sea (southwest Pacific Ocean), *Geology*, 21(6), 555–558, doi:10.1130/0091-7613(1993)021<0555:TTBTBP>2.3.CO;2, 1993.
- 690 Lauretano, V., Kennedy-Asser, A. T., Korasidis, V. A., Wallace, M. W., Valdes, P. J., Lunt, D. J., Pancost, R. D. and Naafs, B. D. A.: Eocene to Oligocene terrestrial Southern Hemisphere cooling caused by declining $p\text{CO}_2$, *Nat. Geosci.*, doi:10.1038/s41561-021-00788-z, 2021.
- Lear, C. H., Bailey, T. R., Pearson, P. N., Coxall, H. K. and Rosenthal, Y.: Cooling and ice growth across the Eocene-Oligocene transition, *Geology*, 36(3), 251–254, doi:10.1130/G24584A.1, 2008.
- 695 Lee, D. E., Lee, W. G., Jordan, G. J. and Barreda, V. D.: The Cenozoic history of New Zealand temperate rainforests: comparisons with southern Australia and South America, *New Zeal. J. Bot.*, 54(2), 100–127, doi:10.1080/0028825X.2016.1144623, 2016.
- Legendre, P. and Legendre, F.: *Numerical Ecology*, 3rd ed., Elsevier., 2012.
- Liu, Z., Pagani, M., Zinniker, D., DeConto, R., Huber, M., Brinkhuis, H., Shah, S. R., Leckie, R. M. and Pearson, A.: Global cooling during the Eocene-Oligocene climate transition, *Science*, 323(5918), 1187–1190, doi:10.1126/science.1166368, 2009.
- 700 López-Quirós, A., Escutia, C., Etourneau, J., Rodríguez-Tovar, F. J., Roignant, S., Lobo, F. J., Thompson, N., Bijl, P. K., Bohoyo, F., Salzmann, U., Evangelinos, D., Salabarnada, A., Hoem, F. S. and Sicre, M. A.: Eocene-Oligocene paleoenvironmental changes in the South Orkney Microcontinent (Antarctica) linked to the opening of Powell Basin, *Glob. Planet. Change*, 204, doi:10.1016/j.gloplacha.2021.103581, 2021.
- Mabberley, D. J.: *The Plant-Book*, Second., Cambridge University Press., 1997.
- 705 Macphail, M. K.: Palynostratigraphy of the murray basin, inland Southeastern Australia, *Palynology*, 23(1), 197–240, doi:10.1080/01916122.1999.9989528, 1999.
- Macphail, M. and Cantrill, D. J.: Age and implications of the Forest Bed, Falkland Islands, southwest Atlantic Ocean: Evidence from fossil pollen and spores, *Palaeogeogr. Palaeoclimatol. Palaeoecol.*, 240(3–4), 602–629, doi:10.1016/j.palaeo.2006.03.010, 2006.
- 710 Macphail, M., Alley, F., Truswell, E. and Sluiter, I. R. K.: Early Tertiary vegetation: Evidence from spores and pollen, in *History of the Australian Vegetation: Cretaceous to Recent*, edited by R. S. Hill, pp. 189–261, Cambridge University Press,

- Cambridge., 1994.
- Macphail, M. K.: Australian Palaeoclimates: Cretaceous to Tertiary - A review of palaeobotanical and related evidence to the year 2000, CRC LEME Spec. Vol. Open File Rep. 151, (November), 266pp, 2007.
- 715 Macphail, M. K. and Hill, R. S.: What was the vegetation in northwest Australia during the Paleogene, 66–23 million years ago?, *Aust. J. Bot.*, 66(7), 556–574, doi:10.1071/BT18143, 2018.
- Macphail, M. K. and Truswell, E. M.: Palynology of Site 1166, Prydz Bay, East Antarctica, in *Proceedings of the Ocean Drilling Program, Scientific Results*, vol. 188, edited by A. K. Cooper, P. E. O'Brien, and C. Richter, pp. 1–43, Ocean Drilling Program., 2004.
- 720 Macphail, M. K., Pemberton, M. and Jacobson, G.: Peat mounds of southwest Tasmania: Possible origins, *Aust. J. Earth Sci.*, 46(5), 667–677, doi:10.1046/j.1440-0952.1999.00736.x, 1999.
- Martin, H.: Australian Tertiary phytogeography: Evidence for palynology, in *History of the Australian vegetation: Cretaceous to Holocene*, edited by R. S. Hill, pp. 104–142, Cambridge University Press, Cambridge., 1994.
- Martin, H. A.: Cenozoic climatic change and the development of the arid vegetation in Australia, *J. Arid Environ.*, 66(3 SPEC. ISS.), 533–563, doi:10.1016/j.jaridenv.2006.01.009, 2006.
- 725 Mosbrugger, V.: The nearest living relative method, in *Fossil Plants and Spores: Modern Techniques*, edited by T. P. Jones and N. P. Rowe, pp. 261–265, Geological Society, London., 1999.
- Mosbrugger, V. and Utescher, T.: The coexistence approach - A method for quantitative reconstructions of Tertiary terrestrial palaeoclimate data using plant fossils, *Palaeogeogr. Palaeoclimatol. Palaeoecol.*, 134(1–4), 61–86, doi:10.1016/S0031-0182(96)00154-X, 1997.
- 730 Myerscough, P., Whelan, R. and Bradstock, R.: Ecology of Proteaceae with special reference to the Sydney region, *Cunninghamia*, 6(4), 951–1015, 2007.
- Naafs, B. D. A., Inglis, G. N., Zheng, Y., Amesbury, M. J., Biester, H., Bindler, R., Blewett, J., Burrows, M. A., del Castillo Torres, D., Chambers, F. M., Cohen, A. D., Evershed, R. P., Feakins, S. J., Galka, M., Gallego-Sala, A., Gandois, L., Gray, D. M., Hatcher, P. G., Honorio Coronado, E. N., Hughes, P. D. M., Huguet, A., Könönen, M., Laggoun-Défarge, F., Lähteenoja, O., Lamentowicz, M., Marchant, R., McClymont, E., Pontevedra-Pombal, X., Ponton, C., Pourmand, A., Rizzuti, A. M., Rochefort, L., Schellekens, J., De Vleeschouwer, F. and Pancost, R. D.: Introducing global peat-specific temperature and pH calibrations based on brGDGT bacterial lipids, *Geochim. Cosmochim. Acta*, 208, 285–301, doi:10.1016/j.gca.2017.01.038, 2017.
- 740 Oksanen, J., Blanchet, F. G., Friendly, M., Kindt, R., Legendre, P., McGlenn, D., Minchin, P. R., O'Hara, R. B., Simpson, G. L., Solymos, P., Stevens, M. H. H., Szoecs, E. and Wagner, H.: Vegan: community ecology package, R Packag. version 2.5-6. [online] Available from: <https://cran.r-project.org/package=vegan> (Accessed 9 August 2021), 2019.
- Pagani, M., Huber, M., Liu, Z., Bohaty, S. M., Henderiks, J., Sijp, W., Krishnan, S. and DeConto, R. M.: The role of Carbon dioxide during the onset of Antarctic glaciation, *Science* (80-), 334(6060), 1261–1264, doi:10.1126/science.1203909, 2011.
- 745 Pälike, H., Norris, R. D., Herrle, J. O., Wilson, P. A., Coxall, H. K., Lear, C. H., Shackleton, N. J., Tripathi, A. K. and Wade, B. S.: The heartbeat of the Oligocene climate system, *Science* (80-), 314(5807), 1894–1898, doi:10.1126/science.1133822,

2006.

Partridge, A. and Dettmann, M.: Plant microfossils, in *Geology of Victoria*, edited by W. D. Birch, pp. 639–652, Geological Society of Australia Special Publication., 2003.

750 [Partridge, D. A.: New observations on the Cenozoic stratigraphy of the Bassian Rise derived from a palynological study of the Groper-1, Mullet-1 and Bluebone-1 wells, offshore Gippsland Basin, southeast Australia., 2006.](#)

Passchier, S., Ciarletta, D. J., Miriagos, T. E., Bijl, P. K. and Bohaty, S. M.: An Antarctic stratigraphic record of stepwise ice growth through the Eocene-Oligocene transition, *Bull. Geol. Soc. Am.*, 129(3–4), 318–330, doi:10.1130/B31482.1, 2017.

755 Pearson, P. N., Foster, G. L. and Wade, B. S.: Atmospheric carbon dioxide through the Eocene–Oligocene climate transition, *Nature*, 461(7267), 1110–1113, doi:10.1038/nature08447, 2009.

Pocknall, D. T.: Palynology of Waikato Coal Measures (Late Eocene-late Oligocene) from the Raglan area, North Island, New Zealand, *New Zeal. J. Geol. Geophys.*, 28(2), 329–349, doi:10.1080/00288306.1985.10422231, 1985.

Pocknall, D. T.: Late Eocene to early Miocene vegetation and climate history of New Zealand, *J. R. Soc. New Zeal.*, 19(1), 1–18, doi:10.1080/03036758.1989.10426451, 1989.

760 Pole, M. S. and Macphail, M. K.: Eocene *Nypa* from Regatta Point, Tasmania, *Rev. Palaeobot. Palynol.*, 92, 55–67, 1996.

Pound, M. J. and Salzmann, U.: Heterogeneity in global vegetation and terrestrial climate change during the late Eocene to early Oligocene transition, *Sci. Rep.*, 7(43386), doi:10.1038/srep43386, 2017.

765 Prebble, J. G., Raine, J. I., Barrett, P. J. and Hannah, M. J.: Vegetation and climate from two Oligocene glacioeustatic sedimentary cycles (31 and 24 Ma) cored by the Cape Roberts Project, Victoria Land Basin, Antarctica, *Palaeogeogr. Palaeoclimatol. Palaeoecol.*, 231(1–2), 41–57, doi:10.1016/j.palaeo.2005.07.025, 2006.

Prebble, J. G., Kennedy, E. M., Reichgelt, T., Clowes, C., Womack, T., Mildenhall, D. C., Raine, J. I. and Crouch, E. M.: A 100 million year composite pollen record from New Zealand shows maximum angiosperm abundance delayed until Eocene, *Palaeogeogr. Palaeoclimatol. Palaeoecol.*, 566, doi:10.1016/j.palaeo.2020.110207, 2021.

770 Pross, J.: Paleo-oxygenation in Tertiary epeiric seas: evidence from dinoflagellate cysts, *Palaeogeogr. Palaeoclimatol. Palaeoecol.*, 166, 369–381, doi:10.1016/S0031-0182(00)00219-4, 2001.

Pross, J., Klotz, S. and Mosbrugger, V.: Reconstructing palaeotemperatures for the Early and Middle Pleistocene using the mutual climatic range method based on plant fossils, *Quat. Sci. Rev.*, 19(17–18), 1785–1799, doi:10.1016/S0277-3791(00)00089-5, 2000.

775 Pross, J., Contreras, L., Bijl, P. K., Greenwood, D. R., Bohaty, S. M., Schouten, S., Bendle, J. A., Röhl, U., Tauxe, L., Raine, J. I., Huck, C. E., van de Flierdt, T., Jamieson, S. S. R., Stickley, C. E., van de Schootbrugge, B., Escutia, C., Brinkhuis, H., Brinkhuis, H., Escutia Dotti, C., Klaus, A., Fehr, A., Williams, T., Bendle, J. A. P., Bijl, P. K., Bohaty, S. M., Carr, S. A., Dunbar, R. B., González, J. J., Hayden, T. G., Iwai, M., Jimenez-Espejo, F. J., Katsuki, K., Soo Kong, G., McKay, R. M., Nakai, M., Olney, M. P., Passchier, S., Pekar, S. F., Pross, J., Riesselman, C. R., Röhl, U., Sakai, T., Shrivastava, P. K., Stickley, C. E., Sugisaki, S., Tauxe, L., Tuo, S., van de Flierdt, T., Welsh, K., Yamane, M. and Scientists, I. O. D. P. E. 318:
780 Persistent near-tropical warmth on the Antarctic continent during the early Eocene epoch, *Nature*, 488(7409), 73–77, doi:10.1038/nature11300, 2012.

- Quilty, P. G.: Late Eocene foraminifers and palaeoenvironment, Cascade Seamount, southwest Pacific Ocean: Implications for seamount subsidence and Australia Antarctica Eocene correlation, *Aust. J. Earth Sci.*, 48(5), 633–641, doi:10.1046/j.1440-0952.2001.485886.x, 2001.
- 785 R Core Team: R: A language and environment for statistical computing, *R Found. Stat. Comput.* [online] Available from: <https://www.r-project.org/> (Accessed 9 August 2021), 2019.
- Raine, J. C., Mildenhall, D. C. and Kennedy, E. M.: New Zealand fossil spores and pollen: an illustrated catalogue, *GNS Sci. Misc. Ser. no. 4*, 1–25, 2011.
- 790 Read, J. and Hill, R. S.: Dynamics of *Nothofagus*-dominated rainforest on mainland Australia and lowland Tasmania, *Vegetatio*, 63(2), 67–78, doi:10.1007/BF00032607, 1985.
- Read, J., Hope, G. S. and Hill, R. S.: Phytogeography and climate analysis of *Nothofagus* subgenus *Brassospora* in New Guinea and New Caledonia, *Aust. J. Bot.*, 53(4), 297–312, doi:10.1071/BT04155, 2005.
- Reichgelt, T., West, C. K. and Greenwood, D. R.: The relation between global palm distribution and climate, *Sci. Rep.*, 2–12, doi:10.1038/s41598-018-23147-2, 2018.
- 795 Royer, J. and Rollet, N.: Plate-tectonic setting of the Tasmanian region, *Aust. J. Earth Sci.*, 44(5), 543–560, doi:10.1080/08120099708728336, 1997.
- Sanguinetti, J. and Kitzberger, T.: Patterns and mechanisms of masting in the large-seeded southern hemisphere conifer *Araucaria araucana*, *Austral Ecol.*, 33(1), 78–87, doi:10.1111/j.1442-9993.2007.01792.x, 2008.
- 800 Scher, H. D., Bohaty, S. M., Smith, B. W. and Munn, G. H.: Isotopic interrogation of a suspected late Eocene glaciation, *Paleoceanography*, 29(6), 628–644, doi:10.1002/2014PA002648, 2014.
- Shannon, C. E.: A Mathematical Theory of Communication, *Bell Syst. Tech. J.*, 27(3), 379–423, doi:10.1002/j.1538-7305.1948.tb01338.x, 1948.
- Shipboard Scientific Party: Site 1172, in *Proceedings of the Ocean Drilling Program, 189 Initial Reports*, edited by N. F. Exon, J. P. Kennett, and M. J. Malone, pp. 1–149, *Ocean Drilling Program.*, 2001.
- 805 ~~Stevens, P. F.: *Angiosperm Phylogeny Website, Version 14, July 2017, Page last updated: 09/02/2021* [online] Available from: <http://www.mobot.org/MOBOT/research/APweb/> (Accessed 28 September 2021), 2017.~~
- Stickley, C. E., Brinkhuis, H., Schellenberg, S. A., Sluijs, A., Röhl, U., Fuller, M., Grauert, M., Huber, M., Warnaar, J. and Williams, G. L.: Timing and nature of the deepening of the Tasmanian Gateway, *Paleoceanography*, 19(4), 1–18, doi:10.1029/2004PA001022, 2004.
- 810 Thompson, N., Salzmann, U., López-Quirós, A., Bijl, P. K., Hoem, F. S., Etourneau, J., Sicre, M.-A., Roignant, S., Hocking, E., Amoo, M. and Escutia, C.: Vegetation change across the Drake Passage region linked to late Eocene cooling and glacial disturbance after the Eocene–Oligocene ~~Transition~~*transition*, *Clim. Past Discuss.*, 1–39, 18(2), 209–232, doi:10.5194/cp-2021-84, ~~2021~~*18-209-2022, 2022*.
- 815 Tibbett, E. J., Scher, H. D., Warny, S., Tierney, J. E., Passchier, S. and Feakins, S. J.: Late Eocene record of hydrology and temperature from Prydz Bay, East Antarctica, *Paleoceanogr. Paleoclimatology*, 36(4), doi:10.1029/2020PA004204, 2021.

- Tripathi, S. K. and Srivastava, D.: Palynology and palynofacies of the early Palaeogene lignite bearing succession of Vastan, Cambay Basin, Western India, *Acta Palaeobot.*, 52(1), 157–175, 2012.
- Truswell, E. M.: Vegetation changes in the Australian tertiary in response to climatic and phytogeographic forcing factors, *Aust. Syst. Bot.*, 6(6), 533–557, doi:10.1071/SB9930533, 1993.
- 820 Truswell, E. M. and Macphail, M. K.: Polar forests on the edge of extinction: What does the fossil spore and pollen evidence from East Antarctica say?, *Aust. Syst. Bot.*, 22(2), 57–106, doi:10.1071/SB08046, 2009.
- Utescher, T., Mosbrugger, V. and Ashraf, A. R.: Terrestrial climate evolution in Northwest Germany over the last 25 million years, *Palaios*, 15(5), 430–449, doi:10.2307/3515514, 2000.
- 825 Utescher, T., Bruch, A. A., Erdei, B., François, L., Ivanov, D., Jacques, F. M. B., Kern, A. K., Liu, Y. S. C., Mosbrugger, V. and Spicer, R. A.: The Coexistence Approach-Theoretical background and practical considerations of using plant fossils for climate quantification, *Palaeogeogr. Palaeoclimatol. Palaeoecol.*, 410, 58–73, doi:10.1016/j.palaeo.2014.05.031, 2014.
- Vajda, V., Raine, J. I. and Hollis, C. J.: Indication of global deforestation at the Cretaceous-Tertiary boundary by New Zealand fern spike, *Science* (80-), 294(5547), 1700–1702, doi:10.1126/science.1064706, 2001.
- 830 Veblen, T. T.: Regeneration Patterns in Araucaria araucana Forests in Chile, *J. Biogeogr.*, 9(1), 11–28, doi:10.2307/2844727, 1982.
- Veblen, T. T., Hill, R. S. and Read, J.: The ecology and biogeography of Nothofagus forests, Yale University Press, New Haven., 1996.
- 835 Verma, P., Garg, R., Rao, M. R. and Bajpai, S.: Palynofloral diversity and palaeoenvironments of early Eocene Akri lignite succession, Kutch Basin, western India, *Palaeobiodiversity and Palaeoenvironments*, 100(3), 605–627, doi:10.1007/s12549-019-00388-1, 2020.
- Villa, G., Fioroni, C., Pea, L., Bohaty, S. and Persico, D.: Middle Eocene-late Oligocene climate variability: Calcareous nannofossil response at Kerguelen Plateau, Site 748, *Mar. Micropaleontol.*, 69(2), 173–192, doi:10.1016/j.marmicro.2008.07.006, 2008.
- 840 Villa, G., Fioroni, C., Persico, D., Roberts, A. P. and Florindo, F.: Middle Eocene to Late Oligocene Antarctic glaciation/deglaciation and Southern Ocean productivity, *Paleoceanography*, 29(3), 223–237, doi:10.1002/2013PA002518, 2014.
- Willard, D. A., Donders, T. H., Reichgelt, T., Greenwood, D. R., Sangiorgi, F., Peterse, F., Nierop, K. G. J., Frieling, J. and Schouten, S.: Arctic vegetation, temperature, and hydrology during Early Eocene transient global warming events, *Glob. Planet. Change*, 178, 139–152, doi:10.1016/j.gloplacha.2019.04.012, 2019.
- 845 Zachos, J. C., Quinn, T. M. and Salamy, K. A.: High-resolution (10^4 years) deep-sea foraminiferal stable isotope records of the Eocene-Oligocene climate transition, *Paleoceanography*, 11(3), 251–266, doi:10.1029/96PA00571, 1996.
- Zachos, J. C., Dickens, G. R. and Zeebe, R. E.: An early Cenozoic perspective on greenhouse warming and carbon-cycle dynamics, *Nature*, 451(7176), 279–283, doi:10.1038/nature06588, 2008.
- 850 Zanazzi, A., Kohn, M. J., MacFadden, B. J. and Terry, D. O.: Large temperature drop across the Eocene–Oligocene transition in central North America, *Nature*, 445(7128), 639–642, doi:10.1038/nature05551, 2007.

855

Figure captions

860

Figure 1: (A) Location of East Tasman Plateau (ODP Site 1172; red star) and present-day Tasmania (Quilty, 2001). Tasmania landmass in green, and submerged ODP Site 1172 in grey with water depth of ~2620m. (B) Early Oligocene palaeogeography and palaeoceanography of the Tasmanian Gateway. ODP Site 1172 is marked by black five-pointed star. Surface currents are modified after reconstructions by Stickley et al. (2004). TC = Tasman current, PLC = proto-Leeuwin current, ACountC = Antarctic Counter Current AAG = Australo Antarctic Gulf. Solid red arrows indicate warmer ocean currents from the AAG, and solid blue arrows indicate cooler ocean currents. Arrow size also points to the relative strength of the current. Figure is modified after Hoem et al. (2021)

865

870

Figure 2: Sporomorph assemblages and relative abundance of major sporomorph taxa (Angiosperms, Gymnosperms, Cryptogams) recovered from the late Eocene - early Oligocene of ODP Site 1172. Angiosperms' relative abundance are marked by blue bars, Gymnosperms by red bars, and Cryptogams by green bars. In the Angiosperms group, *Nothofagidites* is further divided into subgenera. These are *Brassospora* (B), *Fuscospora* (F) and *Lophozonia* (L)-types. CONISS ordination constrains our late Eocene – early Oligocene sporomorph assemblages into four distinct pollen zones (PZ 1- PZ 4) or vegetation and climate phases. Age model is after Houben et al. (2019) and Bijl et al. (2021).

875

Figure 3: Sporomorph percentage abundance, diversity and Detrended Correspondence Analysis (DCA) results for ODP Site 1172. Percentage abundance for the major groups (Gymnosperms, Other Angiosperms, *Nothofagus* and Cryptogams) are presented for all samples with pollen counts ≥ 75 grains. The DCA results are derived from the sample scores of Axis-1 (measures sample-to sample variance) and shows four distinct compositional groupings as observed with CONISS for the late Eocene - early Oligocene Site 1172 samples. Diversity is calculated based on Sander's rarefaction analysis with samples rarefied at 75 grains/individuals. The Shannon diversity index (H) and evenness (J) are calculated for all samples with counts ≥ 75 grains. Relative percentage abundance of endemic-Antarctic and protoperidinioid dinoflagellate cyst, magnetostratigraphy and age model after Houben et al. (2019). [Gippsland-basin spore-pollen-zonation-after-Holdgate-et-al.-2017](#).

880

885

Figure 4: Comparison of our sporomorph-based climate estimates, MAAT_{soil} values based on MBT'5me, TEX₈₆-based SST and sample score for DCA Axis 1 from the late Eocene – early Oligocene of ODP Site 1172. Sporomorph-based estimates are based on the use of the nearest living relative (NLR) and probability density function (PDF). The ranges of the climate estimates show the mathematical error and not the real range, which may have been a result of uncertainties associated with the use of the NLR approach. Green broken lines indicate average temperatures for sporomorph-based MATs. Biomarker thermometry data are from Bijl et al. (2021). The ~790 kyr interval corresponding to the EOT (34.44-33.65 Ma; Hutchinson et al., 2021) are marked with orange horizontal bar. Age model after Houben et al. (2019).

890

895 **Figure 5. Comparison of the sporomorph-based MAT in the Tasmanian Gateway region across the EOT and earliest Oligocene to regional and global marine EOT and earliest Oligocene records. (A) Marine benthic foraminiferal calcite $\delta^{18}\text{O}$ record from ODP Site 1218 (Pälike et al., 2006). (B) Marine $\delta^{11}\text{B}$ -derived atmospheric $p\text{CO}_2$ record (Anagnostou et al., 2016). (C) Terrestrial temperature change across the EOT and earliest Oligocene based on our sporomorph-based MATs from ODP Site 1172.**

900 **Table captions**

Table 1: List of sporomorph taxa from the late Eocene to early Oligocene of ODP Site 1172 accompanied by botanical affinities, literature sources, nearest living relatives (NLR) selected for climatic reconstruction, and inferred climate range from (Macphail, 2007).

905 **Table 2: Summary of quantitative species diversity and Axis 1, DCA sample score between the late Eocene to early Oligocene from ODP Site 1172.**

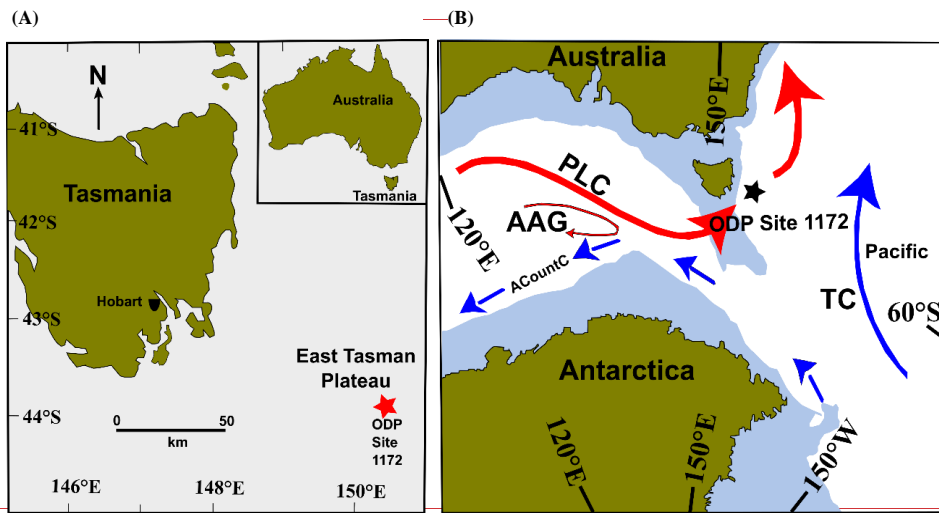
910

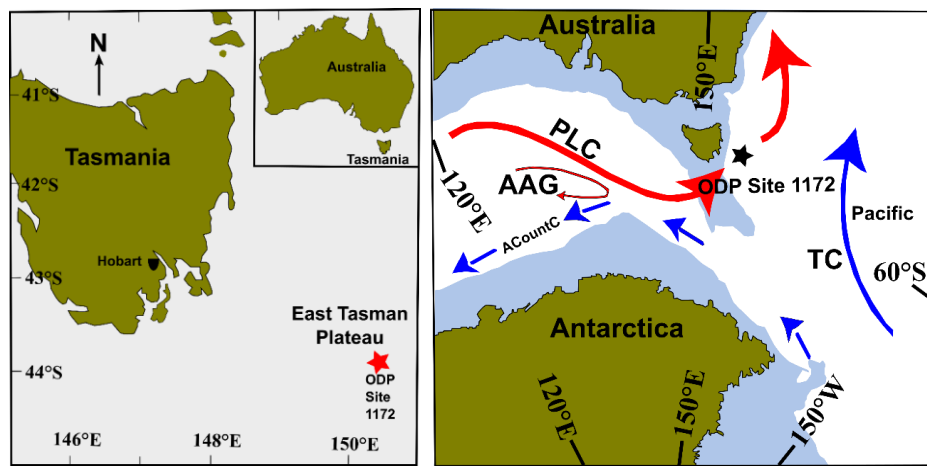
915

920

925

Figure 1.





Formatted: Font color: Auto

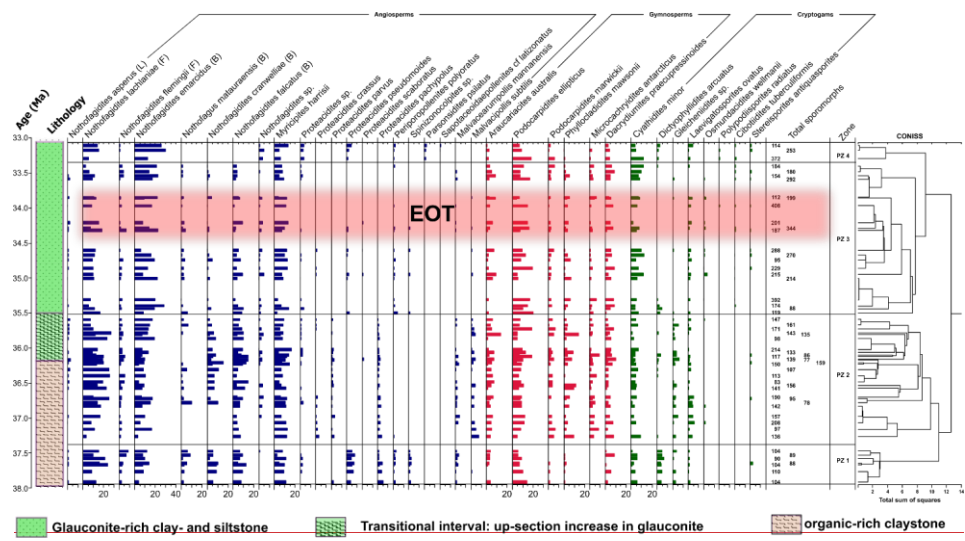
Formatted: Indent: Left: 0 cm, Border: Top: (No border), Bottom: (No border), Left: (No border), Right: (No border), Between : (No border)

940

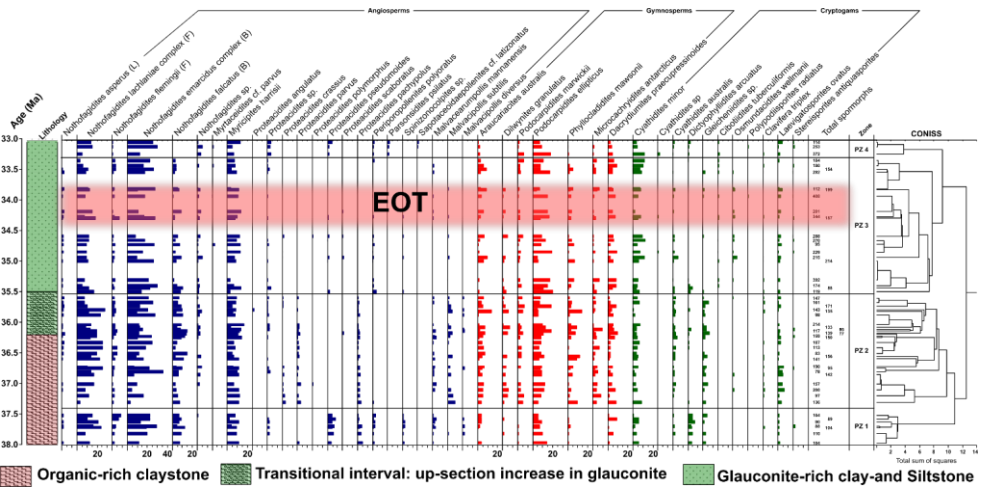
945

950

955 **Figure 2.**



Glauconite-rich clay- and siltstone
 Transitional interval: up-section increase in glauconite
 organic-rich claystone



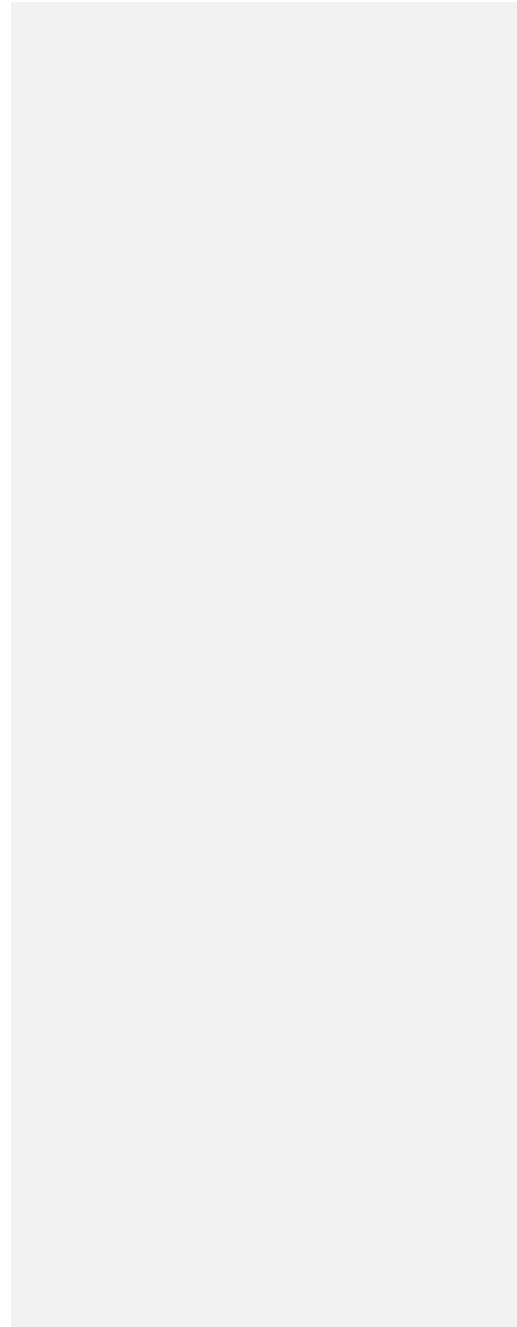
Organic-rich claystone
 Transitional interval: up-section increase in glauconite
 Glauconite-rich clay- and siltstone

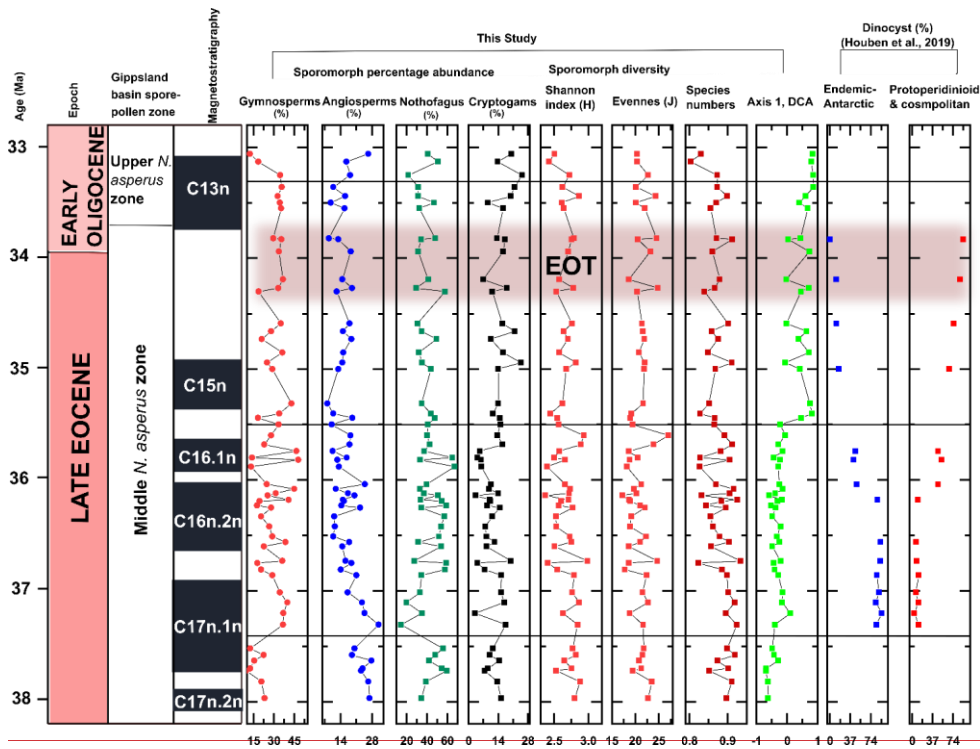
965

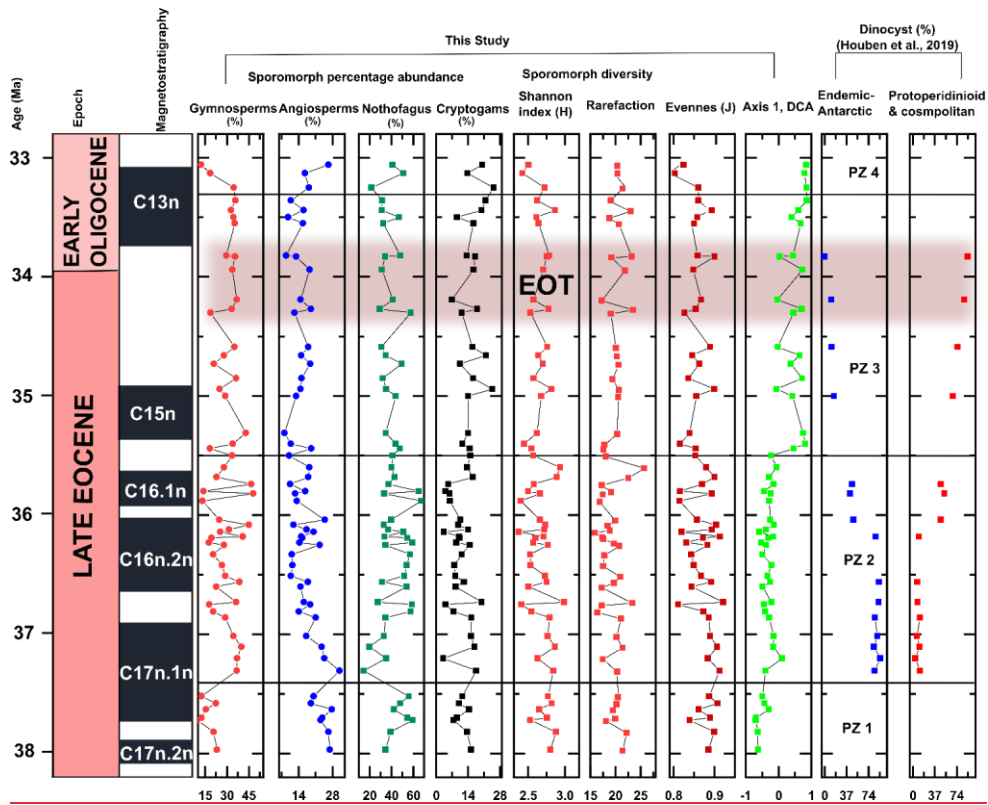
970

975

Figure 3.

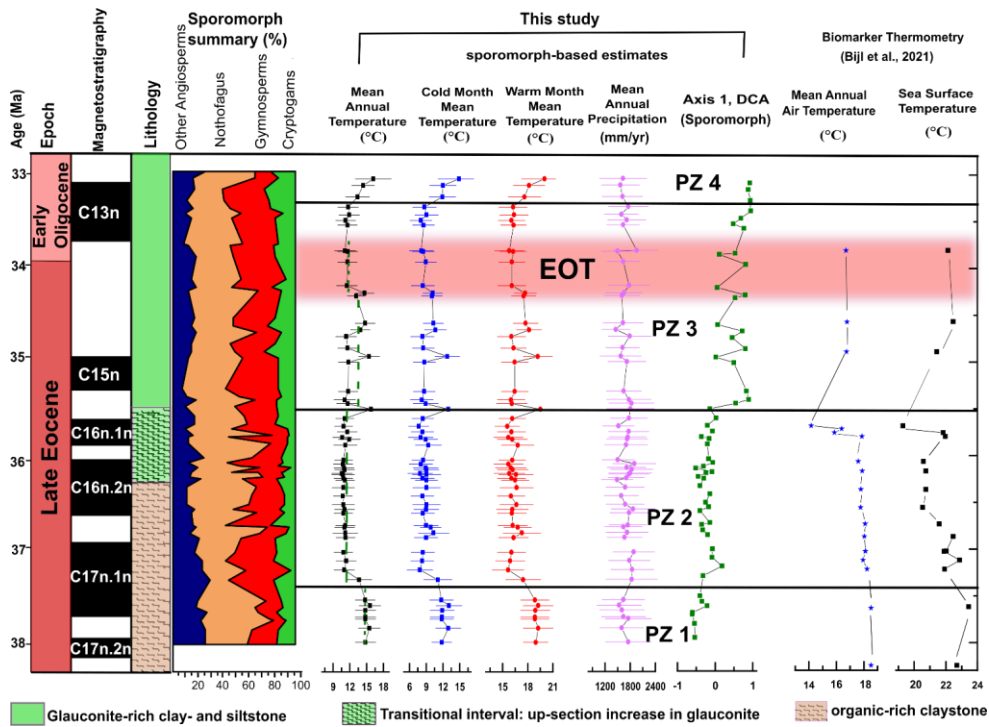






985

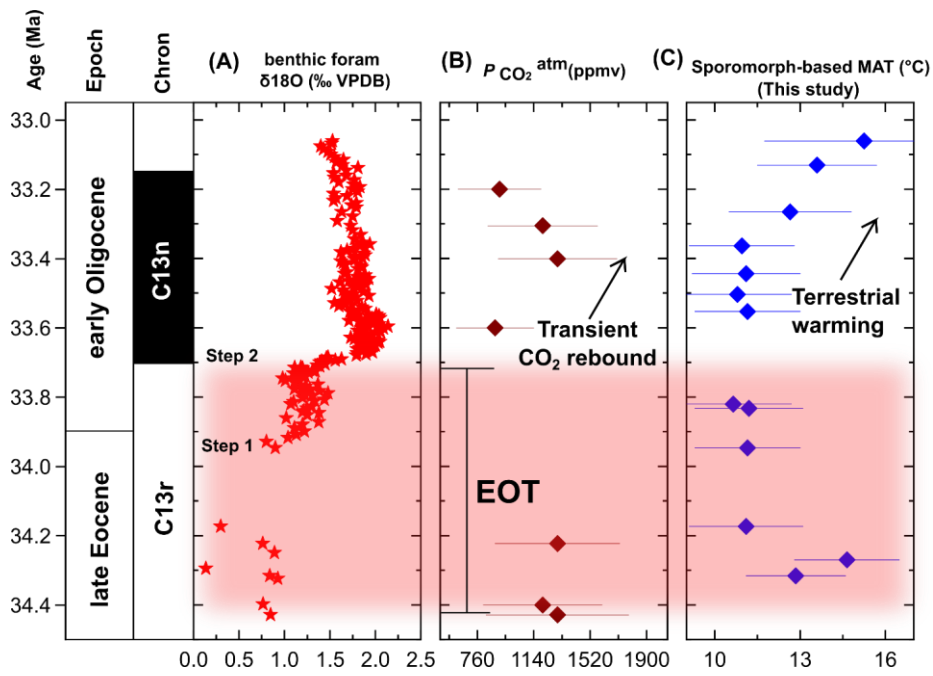
990 **Figure 4.**



995

1000

Figure 5.



1005

1010

1015

Table 1.

Fossil taxon	Botanical Affinity	Source	Selected NLR for climate analysis	Inferred climate Range (Macphail, 2007)
Gymnosperms				
<i>Araucariacites australis</i>	Araucariaceae	Raine et al. (2011)	Araucariaceae	Lower to upper ?mesotherm
<i>Dilwynites granulatus</i>	Araucariaceae	Raine et al. (2011)	Araucariaceae	Lower to upper ?mesotherm
<i>Dacrydiumites preacupressinoides</i>	Podocarpaceae	Raine et al. (2011)	<i>Dacrydium cupressinum</i>	
<i>Podocarpidites ellipticus</i>	Podocarpaceae	Raine et al. (2011)	Podocarpaceae	Microtherm to? megatherm
<i>Podocarpidites</i> spp.	Podocarpaceae	Truswell & Macphail (2009)	Podocarpaceae	Microtherm to ?megatherm
<i>Dacrycarpites australiensis</i>	Podocarpaceae	Truswell & Macphail (2009)	Podocarpaceae	Upper microtherm to lower mesotherm
<i>Podocarpidites marwickii</i>	Podocarpaceae	Raine et al. (2011)	Podocarpaceae	Microtherm to ?megatherm
<i>Phyllocladites mawsonii</i>	<i>Lagarostrobus</i>	Raine et al. (2011)	<i>Lagarostrobus</i>	Upper microtherm to lower mesotherm
<i>Phyllocladites reticulasaccatus</i>	Podocarpaceae	Raine et al. (2011)	Podocarpaceae	
<i>Microcachrydites antarcticus</i>	Podocarpaceae	Raine et al. (2011)	<i>Microcachrys</i>	Upper microtherm to lower mesotherm
<i>Taxodiaceapollenites hiatus</i>	Cupressaceae	Raine et al. (2011)	Cupressaceae	
<i>Microalatiidites</i> sp.	Podocarpaceae	Raine et al. (2011)	Podocarpaceae	Upper microtherm to lower mesotherm
Angiosperms				
<i>Malvacipollis subtilis</i>	Euphorbiaceae	Raine et al. (2011)	Euphorbiaceae	
<i>Myricipites harrisii</i>	Casuarinaceae	Raine et al. (2011) Macphail (2007)	<i>Gymnostoma</i>	Lower mesotherm to megatherm
<i>Nothofagidites flemingii</i>	<i>Nothofagus</i> subg. <i>Fuscospora</i>	Raine et al. (2011)	<i>Nothofagus</i> subg. <i>Fuscospora</i>	Upper microtherm to lower mesotherm
<i>Nothofagidites</i> spp.	<i>Nothofagus</i>	Raine et al. (2011)	<i>Nothofagus</i>	Upper microtherm to lower mesotherm
<i>Nothofagidites emarcidus complex</i>	<i>Nothofagus</i> subg. <i>Brassospora</i>	Truswell & Macphail (2009)	<i>Nothofagus</i> subg. <i>Brassospora</i>	Upper microtherm to lower mesotherm
<i>Nothofagidites falcatus</i>	<i>Nothofagus</i> subg. <i>Brassospora</i>	Raine et al. (2011)	<i>Nothofagus</i> subg. <i>Brassospora</i>	Upper microtherm to lower mesotherm
<i>Nothofagidites lachlaniae complex</i>	<i>Nothofagus</i> subg. <i>Fuscospora</i>	Raine et al. (2011)	<i>Nothofagus</i> subg. <i>Fuscospora</i>	Upper microtherm to lower mesotherm
<i>Nothofagidites matauraensis</i>	<i>Nothofagus</i> subg. <i>Brassospora</i>	Raine et al. (2011)	<i>Nothofagus</i> subg. <i>Brassospora</i>	Upper microtherm to lower mesotherm
<i>Nothofagidites waipawaensis</i>	<i>Nothofagus</i> subg. <i>Fuscospora</i>	Raine et al. (2011)	<i>Nothofagus</i> subg. <i>Fuscospora</i>	Upper microtherm to lower mesotherm
<i>Nothofagidites asperus</i>	<i>Nothofagus</i> subg. <i>Lophozonia</i>	Truswell & Macphail (2009)	<i>Nothofagus</i> subg. <i>Lophozonia</i>	Upper microtherm to lower mesotherm
<i>Nothofagidites eramwelliae</i>	<i>Nothofagus</i> subg. <i>Brassospora</i>	Raine et al. (2011)	<i>Nothofagus</i> subg. <i>Brassospora</i>	Upper microtherm to lower mesotherm
<i>Nothofagidites senectus</i>	<i>Nothofagus</i>	Raine et al. (2011)	<i>Nothofagus</i>	
<i>Nothofagidites brachyspinulosus</i>	<i>Nothofagus</i> subg. <i>Fuscospora</i>	Raine et al. (2011)	<i>Nothofagus</i> subg. <i>Fuscospora</i>	
<i>Proteacidites crassus</i>	Proteaceae	Raine et al. (2011)	Proteaceae	Lower to upper mesotherm
<i>Proteacidites pachypolus</i>	Proteaceae	Macphail & Hill (2018)	Proteaceae	Lower to upper mesotherm
<i>Proteacidites pseudomoides</i>	Proteaceae	Raine et al. (2011)	<i>Carnarvonia</i>	Lower to upper mesotherm
<i>Proteacidites leightonii</i>	Proteaceae	Truswell & Macphail (2009)	Proteaceae	Lower to upper mesotherm
<i>Proteacidites reticulatus</i>	Proteaceae	Truswell & Macphail (2009) Raine et al. (2011)	Proteaceae	Lower to upper mesotherm

Formatted Table

Formatted: Font: Not Italic

Formatted Table

Formatted Table

<i>Proteacidites scaboratus</i>	Proteaceae	Raine et al. (2011)	Proteaceae	Lower to upper mesotherm
<i>Proteacidites similis</i>	Proteaceae	Raine et al. (2011)	Proteaceae	Lower to upper mesotherm
<i>Proteacidites parvus</i>	Proteaceae	Bowman et al. (2014) Raine et al. (2011)	<i>Bellendena</i>	Lower to upper mesotherm
<i>Periporopollenites polyoratus</i>	Caryophyllaceae Trimeniaceae	Raine et al. (2011)	Caryophyllaceae	
<i>Parsonsidites psilatus</i>	<i>Parsonsia</i>	Raine et al. (2011)	<i>Parsonsia</i>	Upper mesotherm to megatherm
<i>Spinizonocolpites</i> sp.	Areaceae	Raine et al. (2011) Kumaran et al. 2011	Areaceae	Lower to upper mesotherm
<i>Tricolpites trioblatus</i>	Scrophulariaceae Convolvulaceae	Raine et al. (2011)	<i>Hebe</i>	
<i>Malvacearumpollis mannanensis</i>	Malvaceae	Raine et al. (2011)	Malvaceae	Upper mesotherm to megatherm
<i>Nupharipollis mortonensis</i>	Araceae	Raine et al. (2011)	<i>Nuphar</i>	
<i>Sapotaceoidaepollenites cf latizonatus</i>	Nymphaeaceae Sapotaceae	Raine et al. (2011)	Sapotaceae	
Cryptogams				
<i>Cyathidites australis</i>	Cyatheaceae	Raine et al. (2011) Macphail (1994)	Cyatheaceae	Upper microtherm to lower mesotherm
<i>Cyathidites minor</i>	Cyatheaceae	Raine et al. (2011)	Cyatheaceae	Upper microtherm to lower mesotherm
<i>Cyathidites</i> sp.	Cyatheaceae	Raine et al. (2011)	Cyatheaceae	Upper microtherm to lower mesotherm
<i>Laevigatosporites ovatus</i>	Blechnaceae	Raine et al. (2011) Truswell & Macphail (2009)	Blechnaceae	
<i>Osmundacidites wellmanii</i>	Osmundaceae	Raine et al. (2011)	<i>Todea</i>	
<i>Osmundacidites</i> sp.	Osmundaceae	Raine et al. (2011) Raine et al. (2011) Truswell & Macphail (2009)	Osmundaceae	
<i>Baculatisporites comaumensis</i>	Osmundaceae, Hymenophyllaceae	Macphail and Cantrill (2006) Truswell & Macphail (2009)	<i>Hymenophyllum</i>	
<i>Gleicheniidites senonicus</i>	Gleicheniaceae	Raine et al. (2011) Truswell & Macphail (2009)	Gleicheniaceae	
<i>Gleicheniidites</i> spp.	Gleicheniaceae	Raine et al. (2011) Truswell & Macphail (2009)	Gleicheniaceae	
<i>Dictyophyllidites arcuatus</i>	Gleicheniaceae	Raine et al. (2011)	Gleicheniaceae	
<i>Kuyltisporites waterbolkii</i>	Cyatheaceae	Raine et al. (2011)	Cyatheaceae	Upper microtherm to lower mesotherm
<i>Clavifera rudis</i>	Gleicheniaceae	Raine et al. (2011) Raine et al. (2011)	Gleicheniaceae	
<i>Clavifera triplex</i>	Gleicheniaceae	Truswell & Macphail (2009) Truswell & Macphail (2009)	Gleicheniaceae	
<i>Laevigatosporites major</i>	Blechnaceae	Raine et al. (2011) Macphail & Hill (2018)	Blechnaceae	
<i>Stereisporites antiquasporites</i>	Sphagnaceae	Truswell & Macphail (2009)	<i>Sphagnum</i>	± microtherm
<i>Ceratosporites equalis</i>	Selaginellaceae	Raine et al. (2011)	<i>Selaginella</i>	
<i>Cibotiidites tuberculiformis</i>	Schizaeaceae	Raine et al. (2011) Daly et al. (2011)	Schizaeaceae	
<i>Polypodiisporites radiatus</i>	Polypodiaceae	Raine et al. (2011)	Polypodiaceae	
<i>Retriletes austroclavatidites</i>	Lycopodiaceae	Raine et al. (2011)	<i>Lycopodium</i>	

1020

Table 2.

Analysis	Pollen Zone 1		Pollen Zone 2		Pollen Zone 3		Pollen Zone 4	
	<i>Mean</i>	<i>(SD)</i>	<i>Mean</i>	<i>(SD)</i>	<i>Mean</i>	<i>(SD)</i>	<i>Mean</i>	<i>(SD)</i>
Rarefaction (75 individuals)	<u>21.641</u> <u>9.65</u>	1.32	<u>20.5219</u> <u>.44</u>	<u>2.3449</u>	<u>21.3720.15</u>	<u>1.8479</u>	21.16	1.37
Shannon index (H)	<u>2.7557</u>	1.12	<u>2.6656</u>	<u>0.4622</u>	<u>2.6658</u>	<u>0.4012</u>	2.54	0.15
Equitability (J)	<u>0.8985</u>	0.02	<u>0.8886</u>	<u>0.0304</u>	<u>0.8785</u>	0.02	0.83	0.03
DCA (Axis 1, sample scores)	-0.55	0.15	-0.29	0.15	0.44	0.33	0.83	0.03

1025